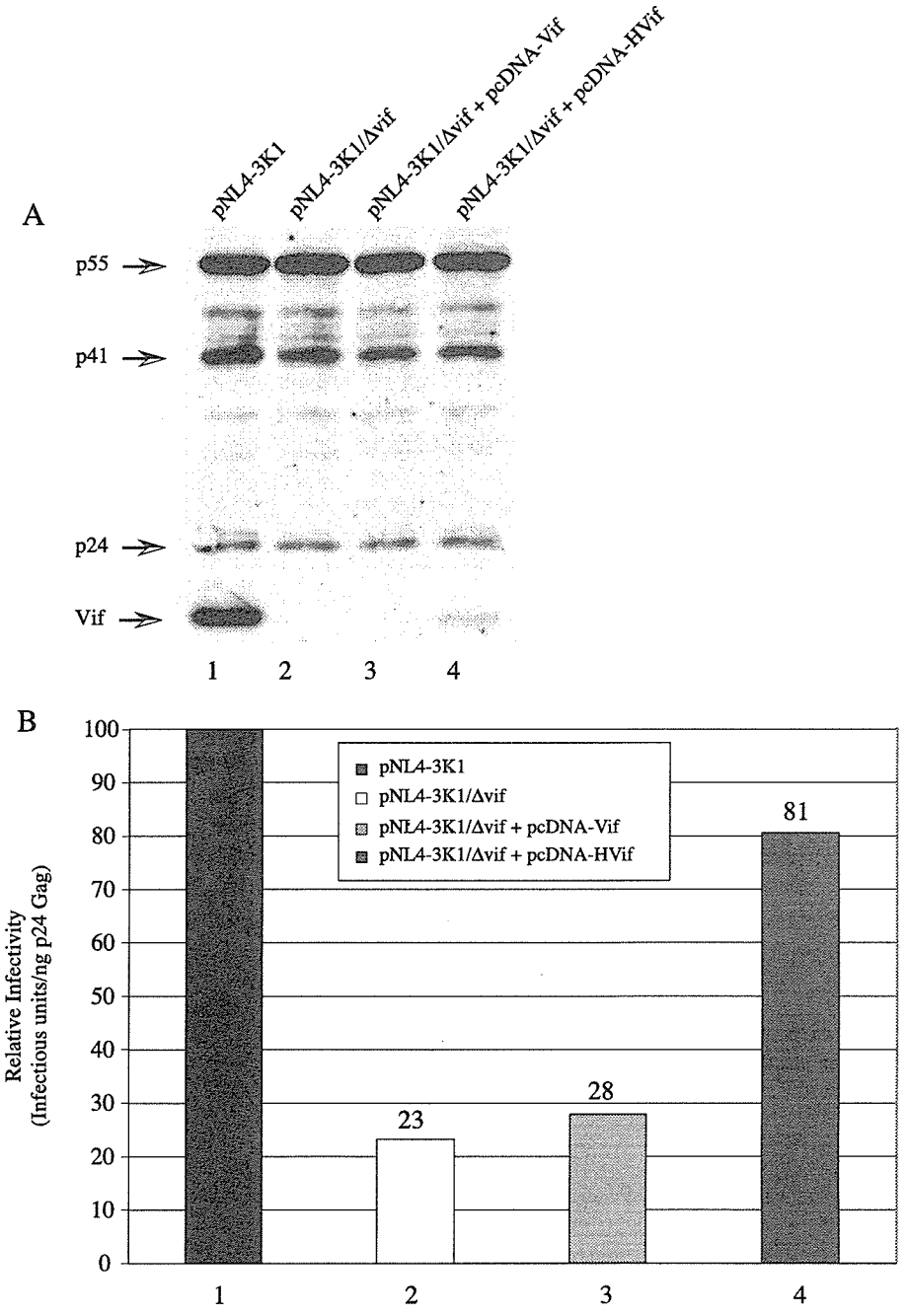

Fig. 3. Biological activity of pcDNA-HVif. (A) Pseudotyped viruses were obtained by transfecting 4×10^6 H9 cells with (lane 1) pNL43-K1, pCMV-G, and pcDNA; (lane 2) pNL43-K1/Δvif, pCMV-G, and pcDNA; (lane 3) pNL43-K1/Δvif, pCMV-G, and pcDNA-vif; (lane 4) pNL43-K1/Δvif, pCMV-G, and pcDNA-HVif (5 mg each, 15 mg in total) by electroporation. Transfected H9 cells were lysed 24 h posttransfection, separated on a 12.5% polyacrylamide-SDS gel, probed with anti-Vif antibody and anti-p24Gag, and visualized by ECL chemiluminescence. The position of the p55, p41, and p24 major Gag products as well as Vif are indicated on the left. (B) Twenty-four hours posttransfection, culture supernatants were harvested, filtered, and quantified by p24 ELISA. Viral infectivity was determined by MAGI assay. Averages of three independent experiments are shown.

protein expression, we first examined the steady-state levels of the respective mRNA. HeLa cells were transfected with plasmids encoding either the native (pcDNA-Vpu) or optimized (pcDNA-Vphu) *vpu* gene. Total and cytoplasmic RNA was extracted, separated by gel electrophoresis and probed in Northern blotting with a 212-nt probe mapping to the 5′ UTR (Fig. 4A). As expected, no *vpu*-specific band was detected in the pcDNA 3.1(−) empty vector control. Interestingly, little or no *vpu*-specific RNA was detected from cells transfected with pcDNA-Vpu, suggesting that the lack of protein expression from this vector is mainly due to its inability to accumulate *vpu*-specific mRNA in the nucleus or cytoplasm. In marked contrast, RNA produced by the codon-optimized pcDNA-Vphu was abundant both in the

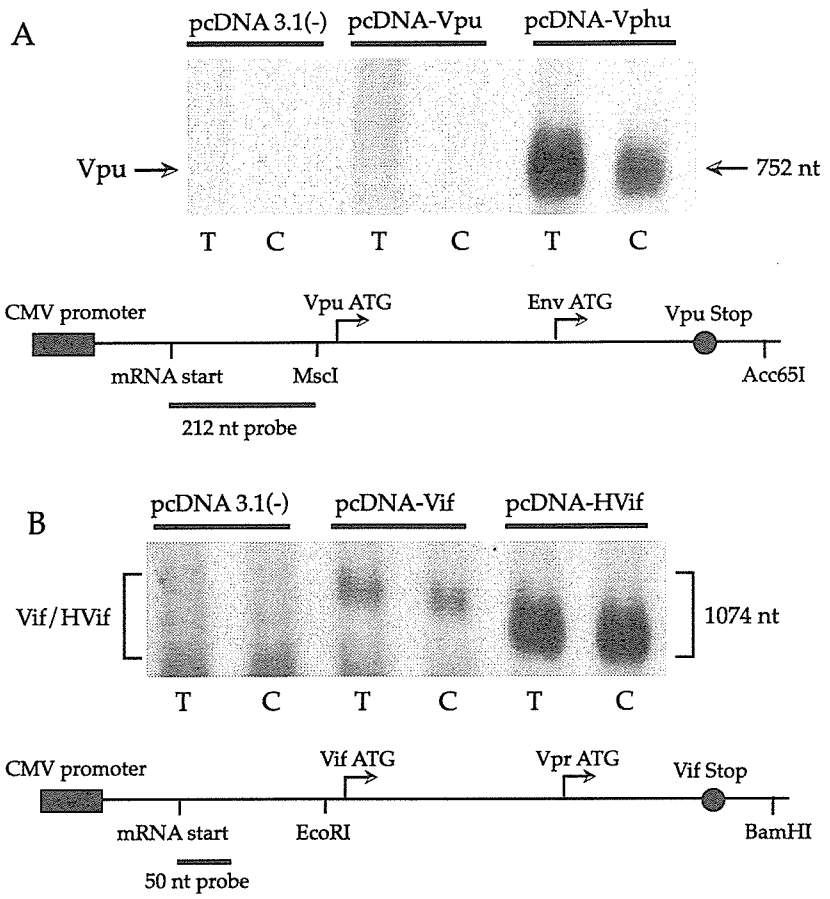

Fig. 4. Effect of codon optimization on RNA steady-state levels. (A) Vpu and Vphu RNA levels. HeLa cells were transfected with 2 μg pcDNA3.1, pcDNA-Vpu, or pcDNA-Vphu. Five micrograms of total and cytoplasmic RNA isolated 24 h posttransfection was separated on a 1% denaturing agarose gel and transferred onto nitrocellulose membrane. A 212-bp biotinylated DNA probe containing sequences complementary to the 5′ UTR of Vpu and Vphu was hybridized to the RNA at 42 °C overnight and detected by chemiluminescence. (B) Comparison of total versus cytoplasmic Vif/HVif RNA levels. HeLa cells were transfected with 2 μg pcDNA3.1, pcDNA-Vif, or pcDNA-HVif. Five micrograms of total and cytoplasmic RNA isolated 24 h posttransfection was separated on a 1% denaturing agarose gel and transferred onto nitrocellulose membrane. A 60-bp biotinylated DNA probe containing sequences complementary to the 5′ UTR of Vif and HVif was hybridized to the RNA at 37 °C overnight and detected by chemiluminescence.

total and cytoplasmic fractions. Similar experiments were performed for the optimized *vif* gene (Fig. 4B). In the case of *vif*, low RNA expression could be detected from the non-optimized pcDNA-Vif construct. However, as was the case for *vpu*, a significant enhancement of both total and cytoplasmic RNA levels was observed following codon optimization (Fig. 4B, pcDNA-HVif). These data strongly suggest that the main effect of codon optimization of both the *vpu* and *vif* genes is at the RNA level whereby higher cytoplasmic mRNA steady-state levels could account for most of the observed increase in protein levels.

To rule out the possibility that the lack of RNA expression from the non-optimized species was due to low transfection efficiency or instability of the plasmid DNA, Southern blots were performed with low molecular weight DNA from cells transfected with both the authentic and codon-optimized Vpu-expressing constructs. No difference was observed in the nuclear accumulation of the pcDNA-Vpu and pcDNA-Vphu plasmids, indicating that both constructs were properly transfected and had similar stability in cells (data not shown).

Effect of codon optimization on transcriptional initiation and elongation

To better define the mechanism by which codon optimization enhances the steady-state levels of *vpu* mRNA, we performed nuclear run-on (NRO) experiments to assess the rate of initiation and elongation of the *vpu* message. To provide a global view of the transcriptional process, multiple DNA probes were used that spanned the entire *vpu* RNA. As shown in Fig. 5A, three separate probes were designed for the *vpu* and *vphu* messages. The 5′ UTR probe spans the transcriptional initiation site and provides a measure of the early transcription events. The 5′ and 3′ coding probes allowed us to monitor the elongation efficiency of the transcribed RNA and assess whether premature termination was occurring. A probe mapping to the

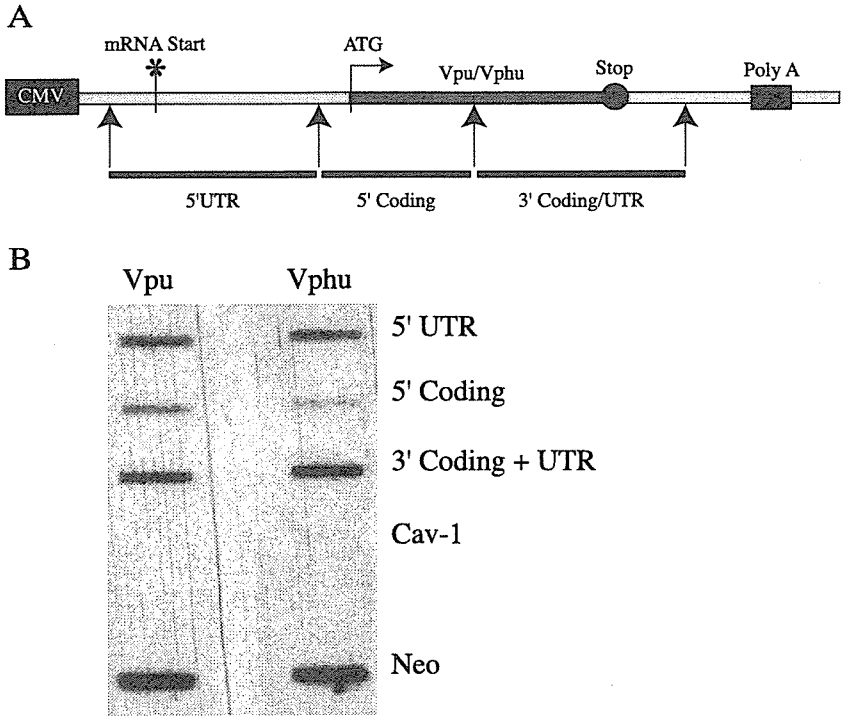

Fig. 5. Transcriptional rate of wild-type and codon-optimized *vpu* genes. (A) Schematic representation of the three cDNA probes used to detect the *vpu* and *vphu* mRNAs. (B) 293T cells were transfected with 2 μg of pcDNA-Vpu and pcDNA-Vphu and 24 h later nuclei were isolated and used in nuclear run-on assays. Nuclei were ^{32}P-labeled in vitro and hybridized to nylon membranes blotted with cDNA fragments diagramed in A. cDNA from an unrelated cellular gene (*caveolin-1*) was used as a control for specificity, and a probe for the neomycin resistance gene was used for transfection and loading controls.

neomycin resistance (*neo*) gene, present in both the pcDNA-Vpu and pcDNA-Vphu constructs served as an internal control for transfection efficiency. Cells were transfected with pcDNA-Vpu or pcDNAVphu, nuclei were isolated, and NROs were performed as described in Materials and methods. Nylon membranes were blotted with the various probes described in Fig. 5A and hybridized with 100,000 cpm of radiolabeled RNA from the NRO reactions. An unrelated cellular gene cDNA (*caveolin-1*) was used as a control for specificity and a probe for the *neo* gene was used for transfection and loading controls. As shown in Fig. 5B, RNA encoding the non-optimized Vpu was readily detectable, in contrast to the situation observed with steady-state Northern blots (see Fig. 4). In addition, all the intermediates of the full-length *vpu* mRNA, from the 5′ to the 3′ UTRs, were detected, indicating proper initiation and elongation of the non-optimized message (Fig. 5B, Vpu). Similar results were obtained when a probe spanning the complete coding region for these genes were used (data not shown). Results of the NRO also indicated that codon optimization of the *vpu* ORF did not lead to a detectable improvement in the rate of initiation or elongation of the *vphu* message (Fig. 5B, Vphu). The variations in relative intensity between probes for the same gene product are likely due to differences in affinity between the probes rather than a direct measure of the abundance of the different species of RNA. Taken together, these data show that the higher steady-state levels of *vphu* RNA observed after codon optimization are not due to enhanced transcriptional initiation or elongation.

Codon optimization increases the nuclear stability of the Vpu mRNA

Results from the NRO experiments showed that neither the initiation nor the elongation of the *vpu* RNA were affected by codon optimization. Therefore, our inability to detect steady-state levels of *vpu* RNA is likely due to nuclear or translation-coupled degradation of the mRNA. To differentiate between these two possibilities, we performed Northern blot analysis of the *vpu* and *vphu* RNA in cellular RNA fractions using a full-length probe spanning the entire transcribed RNA to detect degradation products. In the case of *vphu*, a discrete band corresponding to the full-length mRNA was detected in both the nuclear (Fig. 6, Vphu, N) and cytoplasmic fractions (Fig. 6, Vphu, C). In addition, a large proportion of the *vphu* RNA was isolated from the cytoplasmic fraction, indicating efficient nuclear export. In sharp contrast, no discrete band corresponding to full-length *vpu* RNA was detected in the nuclear or cytoplasmic fractions (Fig. 6, Vpu). Instead, a smear corresponding to products in various stages of degradation was detected in the nuclear fraction (Fig. 6, Vpu, N). Moreover, the smear was absent in the cytoplasmic fraction, indicating that the bulk of the degradation occurred in the nucleus and that no full-length or partial *vpu* RNA was exported to the cytoplasm

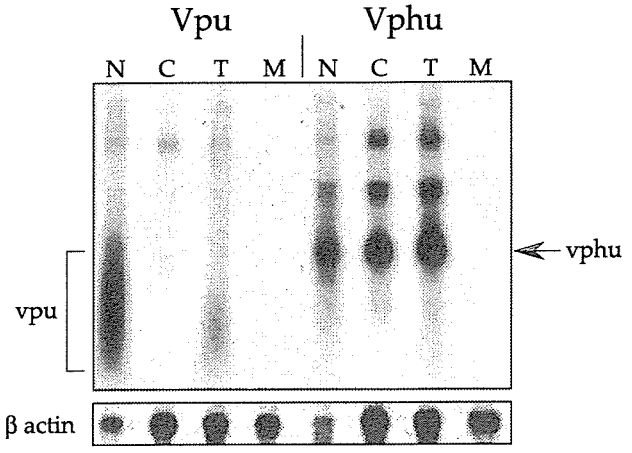

Fig. 6. Subcellular distribution of steady-state levels of *vpu* and *vphu* mRNA. 293T cells were transfected with 2 μg of pcDNA-Vpu and pcDNA-Vphu and 24 h later total RNA was extracted from nuclear (N) and cytoplasmic (C) fractions or unfractionated cells (T) and analyzed by Northern blotting with ^{32}P-labeled Vpu and Vphu cDNA probes. RNA from mock-transfected cells (M) and β-actin were used as a control for specificity and loading, respectively.

(Fig. 6, Vpu, C). These shorter *vpu* mRNA products could account for the signal detected in the NRO experiments of pcDNA-*vpu* transfected cells. Also, longer forms of *vphu* mRNA and a small amount of *vpu* mRNA were detected in the cytoplasmic fractions. These products could represent read-through of the poly A signal in pcDNA3. Taken together, these data allow us to conclude that non-optimized *vpu* fails to express Vpu protein in the absence of Rev because of a lack of cytoplasmic export as well as nuclear degradation of its mRNA. Codon optimization relieves this block by stabilizing the RNA in the nucleus and allowing its efficient export to the cytoplasm.

The codon-optimized vphu message uses a CRM1-independent nuclear export pathway

One possible explanation for the nuclear instability of the non-optimized *vpu* mRNA is that the RNA is not efficiently exported from the nucleus where its prolonged presence leads to enhanced degradation. The ability of the codon-optimized *vpu* message to utilize a different nuclear export pathway would explain the results presented in Fig. 6 and provide a mechanistic explanation for the drastic effect of codon optimization on Vpu expression. It has been reported that Rev-dependent HIV-1 mRNAs such as the *gag* mRNA use the CRM1 Ran-GTP nuclear export pathway and that inhibiting CRM1 function with the drug leptomycin B (LMB) has a pronounced negative effect on the nuclear export of Rev-dependent HIV RNA (Graf et al., 2000; Wolff et al., 1997). We therefore examined the effect of LMB treatment on the rate of Vpu synthesis. Vpu was expressed from its native ORF in a Rev-dependent context from the pNL-A1 construct. The pNL-A1 plasmid also expresses the *env* gene, providing an internal control for another Rev-dependent message. Vphu was expressed from pcDNA-Vphu in the absence of Rev. Twenty-four hours posttransfection, cells were divided into three identical aliquots and pretreated with 0, 10, or 25 nM LMB at 37°C for 2 h. Cells

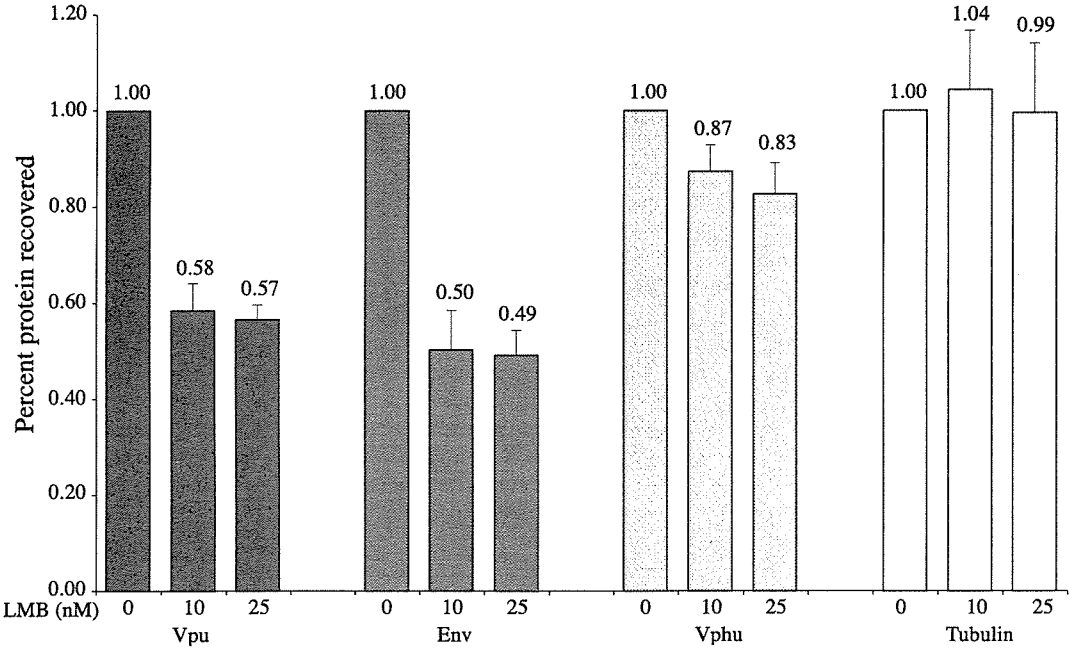

Fig. 7. Effect of LMB treatment on Vpu synthesis. HeLa cells were transfected with 9 μg pNL-A1 (Env and Vpu) or 3 μg pcDNA-Vphu (Vphu). Cells were divided into three equal aliquots and incubated with 0, 10, or 25 nM LMB for 2 h at 37°C. Cells were labeled with [^{35}S]-methionine for 1.5 h at 37°C in the presence or absence of LMB. Cell lysates were immunoprecipitated with antibodies against Vpu, Env, or tubulin, separated by SDS-PAGE, and visualized by fluorography. Bands were quantified and plotted as the ratio of LMB-treated versus untreated control.

were then metabolically labeled for 90 min with [^{35}S]-methionine in the presence or absence of the indicated amounts of LMB. Cell lysates were immunoprecipitated with antibodies to Vpu, Env, or tubulin, separated by SDS-PAGE, and visualized by fluorography (not shown). Bands were quantified with a Bio-Image analyzer and plotted as shown in Fig. 7. As expected, LMB treatment had a significant negative effect on the synthesis of the Rev-dependent Env protein, leading to a 50% reduction in Env protein synthesis during the 90-min labeling (Fig. 7, Env). A similar decrease was observed for Vpu when produced in the context of the pNL-A1 plasmid bearing the native *vpu* ORF (Fig. 7, Vpu). In contrast, LMB had little effect on the synthesis of Vpu when expressed from the codon-optimized pcDNA-Vphu plasmid, even at the highest LMB concentration used (Fig. 7, Vphu). As an internal control, we also examined the synthesis of the cellular tubulin gene both in cells transfected with either pNL-A1 or pcDNA-Vphu. As shown in Fig. 7, tubulin synthesis was unaffected by the presence of LMB, further demonstrating that the effect of the drug was specific for CRM1-dependent RNAs and not the result of general toxicity (Fig. 7, Tubulin). These data indicate that codon optimization of the *vpu* gene led to an increase in RNA stability and accelerated nuclear export by allowing the *vphu* mRNA to utilize a CRM1-independent nuclear export pathway.

Discussion

This work presents the first example of codon optimization of small HIV-1 accessory genes. We demonstrated that partial or complete codon optimization of the *vpu* and *vif* ORFs led to a dramatic enhancement of protein synthesis in the absence of the viral regulatory proteins Tat and Rev and that this was attributable to higher levels of translatable mRNA in the cytoplasm. In the case of the native *vpu* gene, we further demonstrated that the lack of protein synthesis was due to nuclear retention and degradation of its mRNA. In contrast, the mRNA produced by the codon-optimized gene was stable and efficiently exported to the cytoplasm. One important question that remains to be addressed is whether the native *vpu* message is intrinsically unstable due to the presence of destabilizing sequences or whether degradation is a consequence of the prolonged presence of the RNA in the nucleus. Our experiment using the CRM1 blocker LMB favors the latter hypothesis. Indeed, we showed that, in contrast to the native message, the codon-optimized *vpu* RNA was insensitive to LMB, suggesting a mechanism by which codon optimization relieved a nuclear export block. However, it is also possible that destabilizing sequences were still present in the codon-optimized message but that access to a new nuclear export pathway allowed the RNA to exit the nucleus before a functional degradation complex could be formed. Our codon-optimized constructs should provide ideal tools to study these questions in more details and gain new insight into the mechanisms of Rev-regulated nuclear export and RNA stability. Indeed, the small size of the *vpu* ORF will make it easier than in the case of *gag*, *pol*, or *env* to map RNA sequences involved in nuclear retention and/or RNA degradation.

Among the factors that contribute to RNA instability, a strong emphasis has been placed on the overall AU content of the message and the presence of discrete destabilizing sequences such as AREs (Hollams et al., 2002). AREs vary in size and sequence but often contain AUUUA repeats in or near AU-rich sequences. ARE sequences provide binding sites for a variety of RNA binding proteins that can affect all stages of the RNA life cycle, from transcription to nuclear export to degradation (Hollams et al., 2002). In the case of the HIV-1 *gag* message, a number of factors have been implicated in the poor expression of Gag proteins in the absence of Rev and to account for the enhanced expression following codon optimization. Most prominent among those are the inactivation of discrete INS or the decrease in the overall AU content across the length of the coding sequence (Graf et al., 2000; zur Megede et al., 2000). Yet, it is unlikely that these factors explain our results with *vpu* mRNA because no INS motifs have been defined in *vpu* and no ARE sequences conforming to the AUUUA consensus exist in *vpu*. However, the strategy employed here for the codon optimization of *vpu* resulted in a significant decrease in the AU content of the *vpu* ORF; from 63% for the wild type to 42% for the synthetic *vphu*. Interestingly, a CD4-Vpu chimera, CD4U, which we previously found to express Vpu in a Rev-independent manner when fused to the CD4 ectodomain (Bour et al., 2001), had an AU content of 49%. These data suggest that it may be the overall AU content of an mRNA rather than the presence of defined destabilizing sequence elements in the *vpu* ORF such as ARE that can confer instability to otherwise stable messages. These results further suggest that a threshold of AU content might be key to the ability of a given RNA to avoid nuclear degradation. Alternatively, it is possible that sequences near the 5′ end of a message are the main determinants of RNA stability and that introducing stabilizing CD4 sequences at the 5′ of the *vpu* coding sequence was sufficient to abrogate the negative influence of the *vpu* ORF on RNA stability. While this may be in contrast with the finding that most ARE sequences are located in the 3′ UTR of unstable mRNAs, there is experimental evidence that optimization of the first few codons on the 5′ end of poorly expressed genes contributes the most to the increased protein expression (Humphreys et al., 2000; Kim et al., 1997; Vervoort et al., 2000). The importance of 5′ sequences on RNA stability is further illustrated by our finding that partially optimizing the 5′ end of the *vif* gene was sufficient to stabilize its mRNA and enhance protein production.

Codon-optimized *gag–pol* genes have been used for the construction of lentiviral vectors that can transduce a variety of cell types. In addition to enhanced expression, the optimized synthetic genes offer a higher level of safety from

homologous recombination because they lack the 5′ UTR common to all natural HIV messages and bear minimal sequence homology with the coding region of wild-type genes (Wagner et al., 2000). To minimize the chances of recombination, most recombinant vectors using codon-optimized *gag* or *env* lack accessory genes. While often dispensable for viral propagation in vitro, accessory genes such as *vpu* and *vif* provide important functions during the viral life cycle. The Vpu protein has the ability to enhance the rate of viral particle production while Vif enhances the infectivity of progeny virus produced in restricted cell types. It would therefore be beneficial to include such accessory factors in the design of recombinant therapeutic lentiviruses (Kobinger et al., 1997; Srinivasakumar and Schuening, 1999). The codon-optimized *vpu* and *vif* genes described in this study therefore have the potential to improve the yield and versatility of current retroviral vectors when these are produced from cells that are not permissive for these genes. In addition, the ability to express the *vpu* gene autonomously will allow better fine-tuning of the expression levels, therefore avoiding the toxicity associated with high levels of Vpu expression (Akari et al., 2001; Bour et al., 2001).

Materials and methods

Cell culture and transfection

HeLa and 293T cells were maintained in Dulbecco's modified Eagle's medium containing 10% (v/v) fetal bovine serum (FBS) and supplemented with L-glutamine and antibiotics (penicillin–streptomycin). For transfections, cells were grown to near confluence in 25-cm^2 flasks. Transfections in HeLa cells were performed with TransIT-LT1 (Panvera), according to the manufacturer's instructions. Transfections in 293T cells were performed by the calcium phosphate co-precipitation method, as described previously (Llano et al., 2002). For preparation of pseudotyped virus, H9 cells were transfected by electroporation using a Gene Pulser II (Bio-Rad) with 5 μg each of pNL43-K1 or pNL43-K1Δvif, pNL-A1 or pNL-A1Δvif and pCMV-VSVG. The culture supernatants were harvested 24 h after transfection, filtered through 0.45 μm filters, and concentrated by ultracentrifugation through 20% sucrose for 1 h at 25,000 rpm using an SW41 rotor (Beckman). The infectivity of the pseudotyped viruses obtained was measured by MAGI assay as previously described (Kimpton and Emerman, 1992).

Plasmids

pNLA-1 is a derivative of pNL4-3 (Adachi et al., 1986), lacking the *gag* and *pol* genes but expressing all other viral genes. The pNLA-1/U-del construct is derived from pNLA-1 (Strebel et al., 1987), and carries a deletion that inactivates the *vpu* gene (Bour et al., 1996; Klimkait et al., 1990). pcDNA-Vpu contains the full-length native *vpu* gene from pNL4-3 cloned into the *Eco*RI and *Kpn*I restriction sites of pcDNA 3.1(−) (Invitrogen). pcDNA-Vphu is derived from pcDNA-Vpu and expresses Vpu from the codon-optimized *vpu* sequence (Vphu) cloned into the *Msc*I–*Acc*65I restriction sites. The Vphu gene was constructed by asymmetric PCR using a series of three overlapping oligonucleotide fragments 137, 124, and 106 nt in length, respectively. The Vpu initiation codon was optimized according to the Kozak context rules (Kozak, 1987). To this effect, the C at position +4 was changed to a G, which further required changing the nucleotides at +5 and +6, resulting in a glutamine to valine change at amino acid position 2. Second, a GCCGCC sequence was introduced immediately upstream of the ATG initiation codon. In addition, each *vpu* codon was modified to conform with the reported codon usage of highly expressed human genes (Kotsopoulou et al., 2000). Two valine codons at positions 6 and 13 were not fully optimized to avoid creating additional *Msc*I sites that would have interfered with subsequent cloning. In these cases, the GTC codon for valine was used instead of the more common GTG codon. The internal *env* initiation codon was inactivated by substituting a C for a T at position 211. Lastly, two unique restriction sites were introduced, neither of which changed the Vpu amino acid sequence: an *Age*I at position 165 and an *Afe*I site at position 229. This codon optimization procedure led to a significant decrease in the AU content of the *vpu* ORF; from 63% for the wild type to 42% for the synthetic *vphu*. However, the difference was less pronounced over the entire length of the Vpu-encoding mRNA (54% for the wild type versus 44% for the *vphu* mRNA). pcDNA-Vif was generated by cloning the wild-type Vif gene from pNL4-3 into pcDNA3.1(−) using the *Eco*RI–*Bam*HI restriction sites. pcDNAHVif is the optimized Vif clone containing the partially codon-optimized Vif gene cloned into pcDNA-Vif using the *Eco*RI–*Pfl*MI restriction sites. The HVif gene was constructed by asymmetric PCR as described above for Vphu. The N-terminal 84 of the 191 codons of the *vif* gene were optimized. A unique *Age*I restriction site at position 8 was created in the synthetic gene, preventing the arginine at position 4 from being fully optimized. pROD1014 is a chimeric virus containing the *env* gene from the HIV-2 ROD14 isolate in the context of the ROD10 HIV-2 full-length molecular clone (Bour et al., 1999). Construct pROD1014RK/TA is a double Env mutant of pROD1014 containing an arginine to lysine substitution at position 422 and a threonine to alanine substitution at position 528 (Bour et al., 2003).

Reverse-transcriptase assays

Virus-containing culture supernatants were collected from transfected HeLa cells 24 h posttransfection and cellular debris removed by centrifugation (16,000 × *g*, 1 min). Reverse-transcriptase assays were performed on 10 μl of virus supernatant as described previously (Willey et al., 1988).

Pulse-chase experiments and immunoprecipitations

For pulse-chase experiments, transfected HeLa cells were collected 24 h posttransfection, labeled with Trans-^{35}S-methionine (2 μCi/μl) and subjected to Chase and immunoprecipitation as previously described (Bour et al., 2003).

Western blotting

Cell lysates were prepared from transfected HeLa cells 24 h posttransfection with 1% NP-40 lysis buffer. Five to 10 μg of total proteins was separated on polyacrylamide-SDS gels. Proteins were transferred onto nitrocellulose membranes using an electroblotter (Genomic Solutions) and probed sequentially with either 1:2000 dilution of rabbit anti-Vpu (U2-3) or 1:10,000 dilution of rabbit anti-Vif and 1:4000 dilution of horseradish peroxidase (HRP)-labeled anti-rabbit IgG. For loading controls, the blots were probed sequentially with 1:2000 dilution of mouse anti-α-tubulin and 1:4000 dilution of HRP-labeled anti-mouse IgG. Proteins were visualized using the ECL Western blotting reagent (Amersham).

Isolation of nuclear and cytoplasmic fractions

Nuclear and cytoplasmic fractions were isolated according to the method of Greenberg and Ziff (1984), with minor modifications. Briefly, 293T cells grown in six-well plates were harvested in lysis buffer containing 0.25% NP-40 and incubated in ice for 15 min. Nuclear and cytoplasmic fractions were separated by spinning at 500 × *g* for 5 min. Nuclei were washed once in NP-40 lysis buffer and purity was evaluated by optical microscopy. Usually, greater than 95% purity was obtained. Cytoplasmic fractions were further clarified by spinning at 1200 × *g* for 10 min.

Northern blotting

RNA from nuclear and cytoplasmic fractions and from unfractionated cells were isolated with Trizol (Invitrogen) and treated with 1 unit of RQ1 RNAse-free DNAse (Promega) per microgram of RNA. RNAs (5 μg each) were separated in 1.2% agarose–formaldehyde gels and transferred to nylon membranes. Prehybridization (2 h) and hybridization (overnight) were done at 42 °C in ULTRAhyb buffer (Ambion). Probes (^{32}P-labeled Vpu or Vphu cDNA fragments, or ^{32}P-labeled β-actin antisense oligonucleotide) were used at 10^6 cpm/ml of hybridization buffer. Membranes were washed at room temperature 3 times for 5 min in 2× SSC/0.5% SDS and 2 times for 15 min at 60 °C (Vpu or Vphu probes) or 50 °C (β-actin) in 0.1× SSC/0.5% SDS.

Nuclear run-on

293T cells were transfected with 2 μg of pcDNA-Vphu or pcDNAVpu. Twenty-four hours after transfection, nuclei were isolated as described above and used in nuclear run-on assays. Freshly isolated nuclei corresponding to 3 × 10^6 transfected 293T cells were used per nuclear run-on reaction (Madisen et al., 1998). Unincorporated ^{32}P-UTP was removed using NucAway spin columns (Ambion) and radiolabeled RNA was measured in a TopCount NXT Microplate Scintillation and Luminescence Counter (Packard). Five micrograms of cDNA probes was blotted on nylon membranes after alkali denaturation. Membranes were prehybridized for 2 h and hybridized overnight at 65 °C with 10^5 cpm/ml of in vitro transcribed ^{32}P-RNA, washed with 2× SSC and incubated for 30 min in 2× SSC containing 1 μg/ml of ribonuclease A at 37 °C.

Southern blotting

Low molecular weight DNA was extracted from the nuclear and cytoplasmic fractions of transfected 293T cells by Hirt extraction (Hirt, 1967), separated on 0.8% agarose gels in 1× TAE buffer (1 μg Hirt DNA/lane), alkali denatured, and transferred to nylon membranes. Membranes were prehybridized for 3 h at 42 °C and then hybridized overnight in the presence of 50% formamide with ^{32}P-labeled Vpu or Vphu cDNA fragments (10^6 cpm/ml).

Acknowledgments

The following reagent was obtained through the AIDS Research and Reference Reagent Program, Division of AIDS, NIAID, NIH: Monoclonal Antibody to HIV-1 p24 (No. 71-31) from Dr. Susan Zolla-Pazner. M.L. and E.M.P are supported by NIH AI47536.

References

Adachi, A., Gendelman, H.E., Koenig, S., Folks, T., Willey, R., Rabson, A., Martin, M.A., 1986. Production of acquired immunodeficiency syndrome-associated retrovirus in human and nonhuman cells transfected with an infectious molecular clone. J. Virol. 59, 284–291.

Akari, H., Bour, S., Kao, S., Adachi, A., Strebel, K., 2001. The human immunodeficiency virus type 1 accessory protein Vpu induces apoptosis by suppressing the nuclear factor kappaB-dependent expression of antiapoptotic factors. J. Exp. Med. 194, 1299–1311.

Bour, S., Strebel, K., 1996. The human immunodeficiency virus (HIV) type 2 envelope protein is a functional complement to HIV type 1 Vpu that enhances particle release of heterologous retroviruses. J. Virol. 70, 8285–8300.

Bour, S., Strebel, K., 2000. HIV accessory proteins: multifunctional components of a complex system. Adv. Pharmacol. 48, 75–120.

Bour, S., Schubert, U., Peden, K., Strebel, K., 1996. The envelope glycoprotein of human immunodeficiency virus type 2 enhances viral particle release: a Vpu-like factor?. J. Virol. 70, 820–829.

Bour, S.P., Aberham, C., Perrin, C., Strebel, K., 1999. Lack of effect of cytoplasmic tail truncations on human immunodeficiency virus type 2 ROD env particle release activity. J. Virol. 73, 778–782.

Bour, S., Perrin, C., Akari, H., Strebel, K., 2001. The human immunodeficiency virus type 1 Vpu protein inhibits NF-kappa B activation by interfering with beta TrCP-mediated degradation of Ikappa B. J. Biol. Chem. 276, 15920–15928.

Bour, S., Akari, H., Miyagi, E., Strebel, K., 2003. Naturally occurring amino acid substitutions in the HIV-2 ROD envelope glycoprotein regulate its ability to augment viral particle release. Virology 309, 85–98.

Chang, D.D., Sharp, P.A., 1989. Regulation by HIV Rev depends upon recognition of splice sites. Cell 59, 789–795.

Gottlinger, H.G., Dorfman, T., Cohen, E.A., Haseltine, W.A., 1993. Vpu protein of human immunodeficiency virus type 1 enhances the release of capsids produced by *gag* gene constructs of widely divergent retroviruses. Proc. Natl. Acad. Sci. U.S.A. 90, 7381–7385.

Graf, M., Bojak, A., Deml, L., Bieler, K., Wolf, H., Wagner, R., 2000. Concerted action of multiple *cis*-acting sequences is required for Rev dependence of late human immunodeficiency virus type 1 gene expression. J. Virol. 74, 10822–10826.

Greenberg, M.E., Ziff, E.B., 1984. Stimulation of 3T3 cells induces transcription of the c-*fos* proto-oncogene. Nature 311, 433–438.

Haas, J., Park, E.C., Seed, B., 1996. Codon usage limitation in the expression of HIV-1 envelope glycoprotein. Curr. Biol. 6, 315–324.

Hirt, B., 1967. Selective extraction of polyoma DNA from infected mouse cell cultures. J. Mol. Biol. 26, 365–369.

Hollams, E.M., Giles, K.M., Thomson, A.M., Leedman, P.J., 2002. mRNA stability and the control of gene expression: implications for human disease. Neurochem. Res. 27, 957–980.

Humphreys, D.P., Sehdev, M., Chapman, A.P., Ganesh, R., Smith, B.J., King, L.M., Glover, D.J., Reeks, D.G., Stephens, P.E., 2000. High-level periplasmic expression in *Escherichia coli* using a eukaryotic signal peptide: importance of codon usage at the 5′ end of the coding sequence. Protein Expr. Purif. 20, 252–264.

Jeang, K.T., Xiao, H., Rich, E.A., 1999. Multifaceted activities of the HIV-1 transactivator of transcription, Tat. J. Biol. Chem. 274, 28837–28840.

Kim, Y.S., Risser, R., 1993. TAR-independent transactivation of the murine cytomegalovirus major immediate-early promoter by the Tat protein. J. Virol. 67, 239–248.

Kim, C.H., Oh, Y., Lee, T.H., 1997. Codon optimization for high-level expression of human erythropoietin (EPO) in mammalian cells. Gene 199, 293–301.

Kimpton, J., Emerman, M., 1992. Detection of replication-competent and pseudotyped human immunodeficiency virus with a sensitive cell line on the basis of activation of an integrated beta-galactosidase gene. J. Virol. 66, 2232–2239.

Kjems, J., Askjaer, P., 2000. Rev protein and its cellular partners. Adv. Pharmacol. 48, 251–298.

Klimkait, T., Strebel, K., Hoggan, M.D., Martin, M.A., Orenstein, J.M., 1990. The human immunodeficiency virus type 1-specific protein vpu is required for efficient virus maturation and release. J. Virol. 64, 621–629.

Kobinger, G.P., Mouland, A.J., Lalonde, J.P., Forget, J., Cohen, E.A., 1997. Enhancement of retroviral production from packaging cell lines expressing the human immunodeficiency type 1 VPU gene. Gene Ther. 4, 868–874.

Kotsopoulou, E., Kim, V.N., Kingsman, A.J., Kingsman, S.M., Mitrophanous, K.A., 2000. A Rev-independent human immunodeficiency virus type 1 (HIV-1)-based vector that exploits a codon-optimized HIV-1 *gag–pol* gene. J. Virol. 74, 4839–4852.

Kozak, M., 1987. At least six nucleotides preceding the AUG initiator codon enhance translation in mammalian cells. J. Mol. Biol. 196, 947–950.

Kypr, J., Mrazek, J., 1987. Unusual codon usage of HIV. Nature 327, 20.

Llano, M., Kelly, T., Vanegas, M., Peretz, M., Peterson, T.E., Simari, R.D., Poeschla, E.M., 2002. Blockade of human immunodeficiency virus type 1 expression by caveolin-1. J. Virol. 76, 9152–9164.

Madisen, L., Krumm, A., Hebbes, T.R., Groudine, M., 1998. The immunoglobulin heavy chain locus control region increases histone acetylation along linked c-*myc* genes. Mol. Cell. Biol. 18, 6281–6292.

Maldarelli, F., Martin, M.A., Strebel, K., 1991. Identification of post-transcriptionally active inhibitory sequences in human immunodeficiency virus type 1 RNA: novel level of gene regulation. J. Virol. 65, 5732–5743.

Ritter Jr., G.D., Yamshchikov, G., Cohen, S.J., Mulligan, M.J., 1996. Human immunodeficiency virus type 2 glycoprotein enhancement of particle budding: role of the cytoplasmic domain. J. Virol. 70, 2669–2673.

Schneider, R., Campbell, M., Nasioulas, G., Felber, B.K., Pavlakis, G.N., 1997. Inactivation of the human immunodeficiency virus type 1 inhibitory elements allows Rev-independent expression of Gag and Gag/protease and particle formation. J. Virol. 71, 4892–4903.

Schwartz, S., Felber, B.K., Pavlakis, G.N., 1992. Distinct RNA sequences in the *gag* region of human immunodeficiency virus type 1 decrease RNA stability and inhibit expression in the absence of Rev protein. J. Virol. 66, 150–159.

Schwartz, S., Felber, B.K., Pavlakis, G.N., 1992. Mechanism of translation of monocistronic and multicistronic human immunodeficiency virus type 1 mRNAs. Mol. Cell. Biol. 12, 207–219.

Srinivasakumar, N., Schuening, F.G., 1999. A lentivirus packaging system based on alternative RNA transport mechanisms to express helper and gene transfer vector RNAs and its use to study the requirement of accessory proteins for particle formation and gene delivery. J. Virol. 73, 9589–9598.

Strebel, K., Daugherty, D., Clouse, K., Cohen, D., Folks, T., Martin, M.A., 1987. The HIV 'A' (sor) gene product is essential for virus infectivity. Nature 328, 728–730.

Strebel, K., Klimkait, T., Martin, M.A., 1988. A novel gene of HIV-1, *vpu*, and its 16-kilodalton product. Science 241, 1221–1223.

Vervoort, E.B., van Ravestein, A., van Peij, N.N., Heikoop, J.C., van Haastert, P.J., Verheijden, G.F., Linskens, M.H., 2000. Optimizing heterologous expression in dictyostelium: importance of 5′ codon adaptation. Nucleic Acids Res. 28, 2069–2074.

Wagner, R., Graf, M., Bieler, K., Wolf, H., Grunwald, T., Foley, P., Uberla, K., 2000. Rev-independent expression of synthetic *gag–pol* genes of human immunodeficiency virus type 1 and simian immunodeficiency virus: implications for the safety of lentiviral vectors. Hum. Gene Ther. 11, 2403–2413.

Willey, R.L., Smith, D.H., Lasky, L.A., Theodore, T.S., Earl, P.L., Moss, B., Capon, D.J., Martin, M.A., 1988. In vitro mutagenesis identifies a region within the envelope gene of the human immunodeficiency virus that is critical for infectivity. J. Virol. 62, 139–147.

Wolff, B., Sanglier, J.J., Wang, Y., 1997. Leptomycin B is an inhibitor of nuclear export: inhibition of nucleo-cytoplasmic translocation of the human immunodeficiency virus type 1 (HIV-1) Rev protein and Rev-dependent mRNA. Chem. Biol. 4, 139–147.

zur Megede, J., Chen, M.C., Doe, B., Schaefer, M., Greer, C.E., Selby, M., Otten, G.R., Barnett, S.W., 2000. Increased expression and immunogenicity of sequence-modified human immunodeficiency virus type 1 *gag* gene. J. Virol. 74, 2628–2635.

THE JOURNAL OF BIOLOGICAL CHEMISTRY

Vol. 279, No. 13, Issue of March 26, pp. 12355–12362, 2004
Printed in U.S.A.

High Level Expression of Human Immunodeficiency Virus Type-1 Vif Inhibits Viral Infectivity by Modulating Proteolytic Processing of the Gag Precursor at the p2/Nucleocapsid Processing Site*

Received for publication, November 12, 2003, and in revised form, January 6, 2004
Published, JBC Papers in Press, January 13, 2004, DOI 10.1074/jbc.M312426200

Hirofumi Akari‡§, Mikako Fujita¶, Sandra Kao‡, Mohammad A. Khan‡, Miranda Shehu-Xhilaga‡, Akio Adachi¶, and Klaus Strebel‡‖

From the ‡Laboratory of Molecular Microbiology, NIAID, National Institutes of Health, Bethesda, Maryland 20892-0460, §Tsukuba Primate Center for Medical Science, The National Institute of Infectious Diseases, Ibaraki 305-0843, Japan, and the ¶Department of Virology, The University of Tokushima Graduate School of Medicine, Tokushima 770-8503, Japan

The human immunodeficiency virus type-1 Vif protein has a crucial role in regulating viral infectivity. However, we found that newly synthesized Vif is rapidly degraded by cellular proteases. We tested the dose dependence of Vif in non-permissive H9 cells and found that Vif, when expressed at low levels, increased virus infectivity in a dose-dependent manner. Surprisingly, however, the range of Vif required for optimal virus infectivity was narrow, and further increases in Vif severely reduced viral infectivity. Inhibition of viral infectivity at higher levels of Vif was cell type-independent and was associated with an accumulation of Gag-processing intermediates. Vif did not act as a general protease inhibitor but selectively inhibited Gag processing at the capsid and nucleocapsid (NC) boundary. Identification of Vif variants that were efficiently packaged but were unable to modulate Gag processing suggests that Vif packaging was necessary but insufficient for the production of 33- and 34-kDa processing intermediates. Interestingly, these processing intermediates, like Vif, associated with viral nucleoprotein complexes more rigidly than mature capsid and NC. We conclude that virus-associated Vif inhibits processing of a subset of Gag precursor molecules at the p2/NC primary cleavage site. Modulation of processing of a small subset of Gag molecules by physiological levels of Vif may be important for virus maturation. However, the accumulation of such processing intermediates at high levels of Vif is inhibitory. Thus, rapid intracellular degradation of Vif may have evolved as a mechanism to prevent such inhibitory effects of Vif.

The human immunodeficiency virus type-1 (HIV-1)[1] Vif protein is essential for viral replication in non-permissive cells such as primary CD4+ T lymphocytes and macrophages as well as some T cell lines including H9 and CEM cells (for review, see Refs. 1 and 2). Vif-defective viruses produced from non-permissive cells are defective at an early postentry step of infection and are unable to complete reverse transcription and integration (3–9). In fibroblasts and most T cell lines, however, Vif is not required for the production of infectious HIV-1. This cell type-dependent requirement for Vif implied the involvement of host factor(s). Indeed, the recent identification of CEM15 (APOBEC3G) as a cellular inhibitor of HIV replication (10) confirmed earlier speculations on the existence of an inhibitory factor in non-permissive cell types (11, 12). APOBEC3G was subsequently found to induce hypermutation of the HIV genome by deaminating cytidine residues on the viral minus-strand cDNA resulting in the introduction of guanosine to adenosine mutations in the HIV genome (13–16). Subsequent reports suggested a role of Vif in the inhibition of APOBEC3G packaging into virus particles (17–21). The mechanism of APOBEC3G exclusion from virions, however, remains under investigation. Some reports suggest that Vif induces degradation of APOBEC3G (20, 21), whereas others report an effect on APOBEC3G translation (17, 19) or both (18).

While most current models propose an intracellular interaction of Vif with APOBEC3G, Vif is also packaged into virions. Virus particles produced from acutely infected cells incorporate 30–100 copies of Vif (22). In fact, packaging of Vif is specific and requires the interaction of Vif with the viral genomic RNA and the nucleocapsid (NC) domain of the Gag precursor (23). Moreover, virus-associated Vif is partially cleaved by the viral protease (PR) (24). Interestingly, mutations at the processing site that inhibited Vif processing inhibited Vif function, whereas mutations that did not interfere with Vif processing also did not affect Vif function (24). While these findings suggested an important role of virus-associated Vif in virions (24), its specific role remains under investigation.

In the current study we report that newly synthesized Vif is rapidly degraded in transiently transfected HeLa cells with a half-life of less than 30 min. We found that the presence or absence of APOBEC3G had no significant effect on the degradation kinetics of Vif. Based on recent reports demonstrating an interaction of Vif with APOBEC3G (17, 21, 25), we postulated that Vif enhances viral infectivity in a dose-dependent and saturable manner. Accordingly, increasing levels of Vif were expected to result in an increase in viral infectivity reaching a plateau of maximal infectivity once saturating amounts of Vif were reached or exceeded. Furthermore, increasing the amounts of Vif in permissive cell types was not expected to affect viral infectivity, as virus production in such cell types is Vif-independent due to the lack of APOBEC3G in such cells. As expected, physiological expression of Vif increased viral infec-

* This work was supported in part by a grant from the National Institutes of Health Intramural AIDS Targeted Antiviral Program (to K. S.). The costs of publication of this article were defrayed in part by the payment of page charges. This article must therefore be hereby marked "*advertisement*" in accordance with 18 U.S.C. Section 1734 solely to indicate this fact.

‖ To whom correspondence should be addressed: NIAID, National Institutes of Health, 4/312, 4 Center Dr., MSC 0460, Bethesda, MD 20892-0460. Tel.: 301-496-3132; Fax: 301-402-0226; E-mail: kstrebel@nih.gov.

[1] The abbreviations used are: HIV-1, human immunodeficiency virus type-1; NC, nucleocapsid; CA, capsid; VSV-G, vesicular stomatitis virus glycoprotein G; MA, matrix; CHAPS, 3-[(3-cholamidopropyl)dimethylammonio]-1-propanesulfonic acid; PR, protease.

tivity in non-permissive cell types in a dose-dependent manner. Surprisingly, however, the amounts of Vif required for maximal effect exhibited a narrow window, and further increases in Vif levels did not result in a plateau of maximal viral infectivity but instead increasingly suppressed viral infectivity irrespective of the producer cell type. We investigated the mechanistic basis of this phenomenon and found that Vif suppresses processing of the Gag precursor at the p2/NC primary cleavage site. The resulting accumulation of 33- and 34-kDa Gag intermediates composed of CA-p2-NC and CA-p2-NC-p1 was found to inhibit viral infectivity. These results provide evidence that virus-associated Vif has the ability to interact with Gag precursor molecules and to modulate Gag maturation. However, Gag maturation is a highly ordered process, and accumulation of excessive amounts of processing intermediates due to high level expression of Vif is detrimental to virus infectivity.

EXPERIMENTAL PROCEDURES

Plasmids—The full-length HIV-1 molecular clone pNL4-3 was used for the production of wild type infectious virus (26). Construction of its variants pNL43-K1 (Env-defective) or pNL4-3vif(−) (Vif-defective) was described previously (27, 28). An Env- and Vif-defective variant, pNL43-K1.vif(−), was constructed by introducing a frameshift mutation in *env* at a KpnI site in pNL4-3vif(−). Plasmid pHCMV-G contains the vesicular stomatitis virus glycoprotein G (VSV-G) gene expressed from the immediate early gene promoter of human cytomegalovirus (29) and was used for the production of VSV-G pseudotypes. Construction of the APOBEC3G expression vector pHIV-Apo3G is described elsewhere (19). Expression of APOBEC3G from pHIV-Apo3G is under the control of the HIV-1 long terminal repeat and thus requires Tat for expression. For expression of Vif in *trans*, the subgenomic expression vector pNL-A1 (30) was used. A Vif-defective variant of pNL-A1, pNL-A1vif(−), was used as a control. Vif deletion mutants VifΔD (deletion of residues 23–43), VifΔF (deletion of residues 23–74), and VifΔI (deletion of residues 4–45) were created by two-step PCR amplification. PCR products were column-purified; appropriate pairs were mixed at equimolar ratios and used as templates for a second round of amplification using flanking primers. Final PCR products were cloned into pNL-A1 between the BssHII and EcoRI sites.

Cells—H9 and LuSIV cells were cultured in RPMI 1640 medium supplemented with 10% fetal bovine serum, L-glutamine, and antibiotics. HeLa cells were maintained in complete Dulbecco's modified Eagle's medium supplemented with 10% fetal bovine serum, L-glutamine, and antibiotics.

Transfection and Analysis of Viral Proteins—H9 cells (4×10^6) were transfected by electroporation with 10 μg each of pNL43-K1 or pNL43-K1.vif(−) and 10 μg of pNL-A1 or pNL-A1vif(−). The culture supernatants were harvested 24 h after transfection, filtered through 0.45-μm filters, and concentrated by ultracentrifugation through 20% sucrose for 1 h at 25,000 rpm using an SW41 rotor (Beckman Instruments). Alternatively, HeLa cells (5×10^6) were transfected with 2 μg each of variants of pNL4-3 and pNL-A1 using LipofectAMINE PLUS™ (Invitrogen). Culture supernatants and cells were harvested 24 h later. Cell and viral lysates were analyzed by immunoblotting as described previously (23) using an HIV-1-infected patient serum (APS) and antibodies against Vif (28), NC (kindly provided by Robert Gorelick), reverse transcriptase (Intracell), p24 capsid, and matrix (MA) (provided by S. Zolla-Pazner and P. Spearman, respectively, and obtained through the National Institutes of Health AIDS Research and Reference Reagent Program (31, 32)).

Pulse/Chase Analysis of Vif—Transfected cells were metabolically labeled for 10 min with [^{35}S]methionine (2 mCi/ml; ICN Biomedical, Inc., Costa Mesa, CA). After the labeling, cells were washed once with phosphate-buffered saline to remove free isotope and suspended in complete RPMI containing all amino acids and 10% fetal bovine serum. Cells were incubated for various times at 37 °C as indicated in the text. Cells were then pelleted and stored at −80 °C. Cell pellets were subsequently extracted with CHAPS buffer (50 mM Tris-hydrochloride, pH 8.0, 5 mM EDTA, 100 mM NaCl, and 0.5% (v/v) CHAPS (3-[(3-cholamidopropyl)dimethylammonio]-1-propanesulfonic acid)) supplemented with 0.2% deoxycholate, incubated on ice for 5 min, vortexed, and pelleted for 3 min at 15,000 × *g*. Proteins present in the supernatant were used for immunoprecipitation with a Vif-specific polyclonal antibody (Vif93) (28). Immunoprecipitated proteins were solubilized by boiling in sample buffer and separated by SDS-PAGE. Radioactive bands were visualized by fluorography, and quantitation was performed using a Fuji BAS 2000 Bio-Image analyzer.

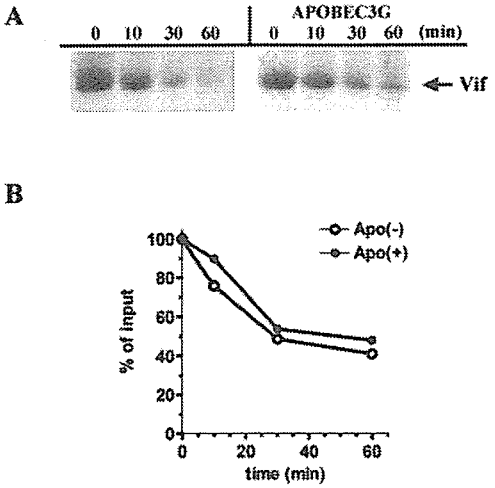

FIG. 1. **Newly synthesized Vif is rapidly degraded.** *A*, HeLa cells were transfected with pNL-A1 (4 μg) and a control vector, pHIV-T4 (1 μg) or pNL-A1 (4 μg) plus pHIV-Apo3G (1 μg). Cells were collected 24 h after transfection, labeled for 10 min with [^{35}S]methionine, and chased for up to 60 min as indicated *above the lanes*. Cell lysates were prepared as described under "Experimental Procedures" and precipitated with a Vif-specific polyclonal antibody. Vif proteins were identified by SDS-PAGE followed by fluorography. *B*, Vif-specific bands shown in *A*, respectively, were quantified using a Fuji BAS 2000 Phospho-Imager. Signals were calculated relative to the input value (time 0 = 100%) and plotted as a function time.

Single-round Viral Infectivity Analysis—Virus stocks derived from transfected H9 or HeLa cells were used for the infection of LuSIV indicator cells (33). To increase the sensitivity of the assay, viruses were pseudotyped with the vesicular stomatitis virus glycoprotein G. Unlike Nef defects, VSV-G pseudotyping does not rescue Vif defects (3, 34). LuSIV cells (5×10^5) were infected in a 24-well plate with 200–400 μl of unconcentrated virus supernatants. Cells were incubated for 24 h at 37 °C. Cells were then harvested and lysed in 150 μl of Promega 1× reporter lysis buffer (Promega Corp., Madison, WI). To determine the luciferase activity in the lysates, 50 μl of each lysate were combined with luciferase substrate (Promega Corp.) by automatic injection, and light emission was measured for 10 s at room temperature in a luminometer (Optocomp II, MGM Instruments, Hamden, CT).

Step Gradient Analysis—Concentrated virus preparations were treated with 0.1% Triton X-100 (final concentration) and subjected to fractionation by centrifugation through a 20%/60% sucrose step gradient as described previously (23). Three equal fractions were collected as depicted in Fig. 5; the top fraction (fraction 1) contains detergent-soluble viral proteins, fraction 2 is a buffer fraction and should not contain significant amounts of any viral proteins, and fraction 3 contains viral core components that are resistant to extraction with Triton X-100. Aliquots of each fraction were analyzed for viral proteins by immunoblotting.

RESULTS

Newly Synthesized Vif Is Rapidly Degraded—Recent work proposed that Vif induces proteasome-dependent degradation of APOBEC3G (20, 21, 25). Although we and others were unable to verify such Vif-dependent degradation of APOBEC3G (17, 19), we nevertheless wanted to assess the possible impact of APOBEC3G on Vif stability. To address this question, we performed pulse/chase analyses in transiently transfected HeLa cells (Fig. 1). To ascertain coexpression of Vif and APOBEC3G in the same cells, Vif was expressed from the subgenomic expression vector pNL-A1 (30), and APOBEC3G was expressed from the Tat-dependent vector pHIV-Apo3G (19). Transfected HeLa cells were labeled for 10 min with [^{35}S]methionine and chased for up to 60 min as described under "Experimental Procedures." As can be seen in Fig. 1*A*, Vif was rapidly degraded both in the absence and presence of

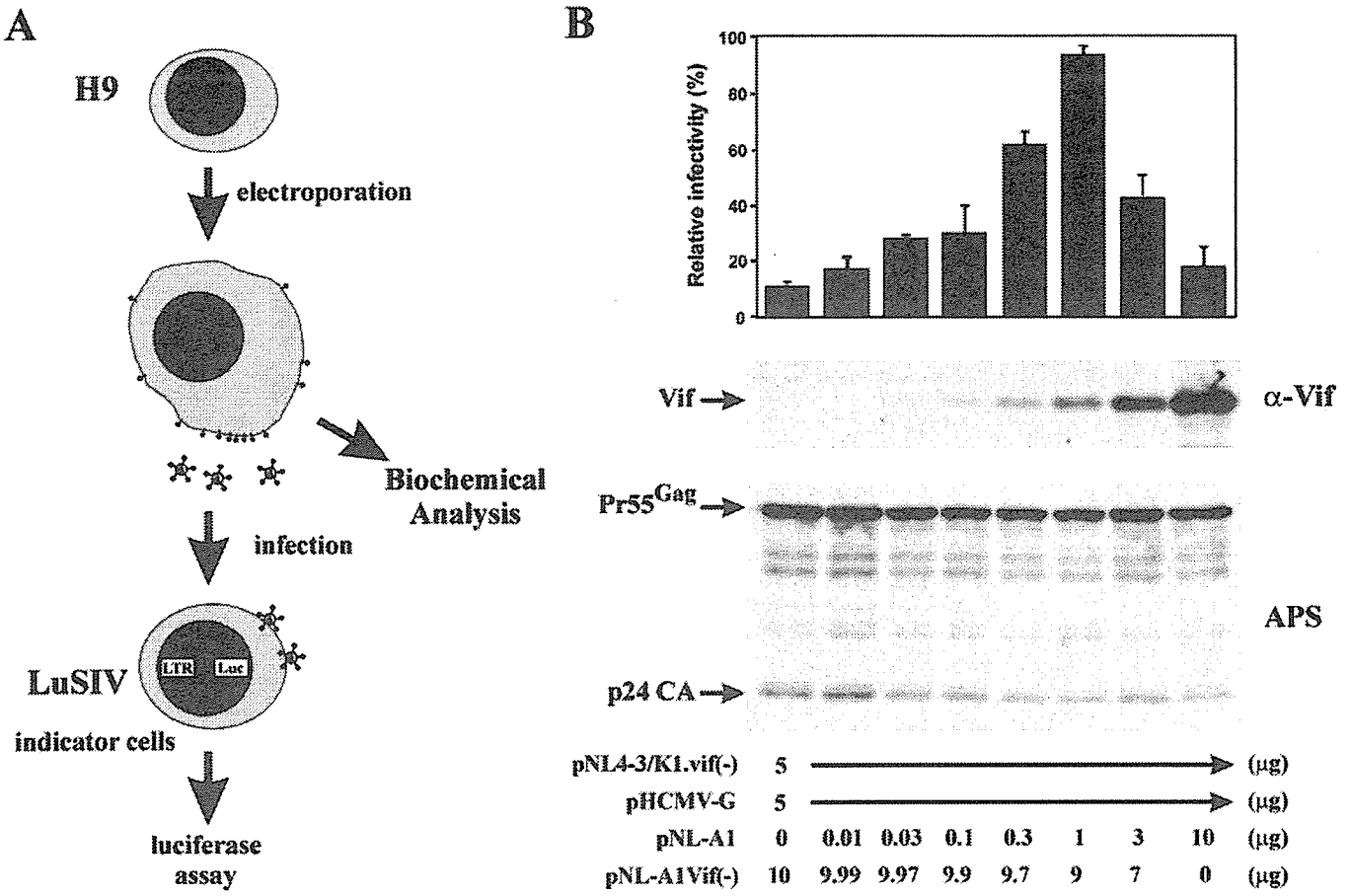

FIG. 2. **Vif is a positive and negative regulator of viral infectivity.** *A*, schematic representation of the experimental procedure. H9 cells are non-permissive and do not support replication of Vif-defective viruses. LuSIV cells are CD4+ indicator cells carrying a luciferase gene under the control of the SIV_{mac239} long terminal repeat (33). *B*, H9 cells were electroporated with constant amounts (5 μg) each of the Vif- and Env-defective pNL43-K1.vif(−) proviral construct and the VSV-G expression vector, pHCMV-G. In addition, increasing amounts of the Vif expression vector pNL-A1 (0–10 μg) were included as indicated at the *bottom*. All samples were adjusted to a total of 20 μg of plasmid DNA using the Vif-defective variant pNL-A1vif(−). Transfected cells and virus-containing supernatants were harvested 24 h after electroporation, and cell lysates were subjected to immunoblot analysis using a Vif-specific antiserum (*α-Vif*) or an HIV-positive patient serum (*APS*). Proteins are identified on the *left*. Virus-containing supernatants were adjusted for equal reverse transcriptase activity (46) and used for the infection of LuSIV indicator cells. Luciferase activity was determined 24 h after infection and used to calculate the relative infectivity of the individual virus stocks (*top*). Maximal infectivity was defined as 100%.

APOBEC3G. Quantitation of the Vif-specific bands (Fig. 1*B*) revealed no difference in the relative decay rates of Vif. Thus, expression of APOBEC3G had no impact on the intracellular stability of Vif. The intracellular site of Vif degradation is under investigation; however, preliminary data suggest the involvement of the cellular proteasome machinery (35).[2]

High Level Expression of Vif in Virus-producing Cells Is Detrimental to HIV-1 Infectivity—The rapid intracellular turnover presumably contributes to the low abundance of Vif in virus-infected cells and limits its packaging into virions. This suggests that Vif may function at very low levels. To determine how much Vif is required for maximal viral infectivity, we examined the dose-dependent effect of Vif on viral infectivity in non-permissive H9 cells. Virus stocks were produced in the presence of increasing amounts of Vif and tested for infectivity in a single-round infection assay. To avoid subsequent rounds of infection, an *env*-defective proviral construct, pNL43-K1.vif(−), was used and pseudotyped with VSV-G. As pNL43-K1.vif(−) is also defective in its *vif* gene, Vif was expressed in *trans* from pNL-A1 (30). This allowed for the controlled expression of increasing amounts of Vif depending on the amounts of pNL-A1 vector transfected. To avoid fluctuations in transfection efficiencies all DNA amounts were equalized by addition of appropriate amounts of a Vif-defective variant of pNL-A1, pNL-A1vif(−). Cells transfected with constant amounts (5 μg) of pNL43-K1.vif(−) as well as pHCMV-G (5 μg) and increasing amounts of pNL-A1 (0.01–10 μg) were harvested 24 h after electroporation. Cell lysates and virus-containing supernatants were used for biochemical characterization as well as for the infection of LuSIV indicator cells as illustrated in Fig. 2*A*. LuSIV cells were collected 24 h after infection, and luciferase activity in the cell lysates was measured as described under "Experimental Procedures." Luciferase activity was normalized for input virus and expressed as percentage of the activity observed for a Vif-expressing control virus, which was defined as 100% (Fig. 2*B*). At low expression levels, Vif enhanced virus infectivity in a dose-dependent manner reaching a peak of infectivity at 1 μg of cotransfected pNL-A1 plasmid DNA. Surprisingly, however, viral infectivity did not plateau with further increases in Vif, but instead higher levels of Vif resulted in a rapid drop in virus infectivity. In fact, at the highest concentration tested (10 μg of pNL-A1 plasmid), the infectivity of the resulting virus was comparable with that of Vif-defective virus. Western blot analysis confirmed that the levels of Vif expression were directly correlated with the amounts of pNL-A1 plasmid transfected (Fig. 2*B*, *α-Vif*) and that increasing Vif expression did not significantly affect Gag expression (Fig. 2*B*, *APS*). These results demonstrate that the level of Vif required for maximal infectivity has a very narrow optimum and that both

[2] M. Fujita, manuscript in preparation.

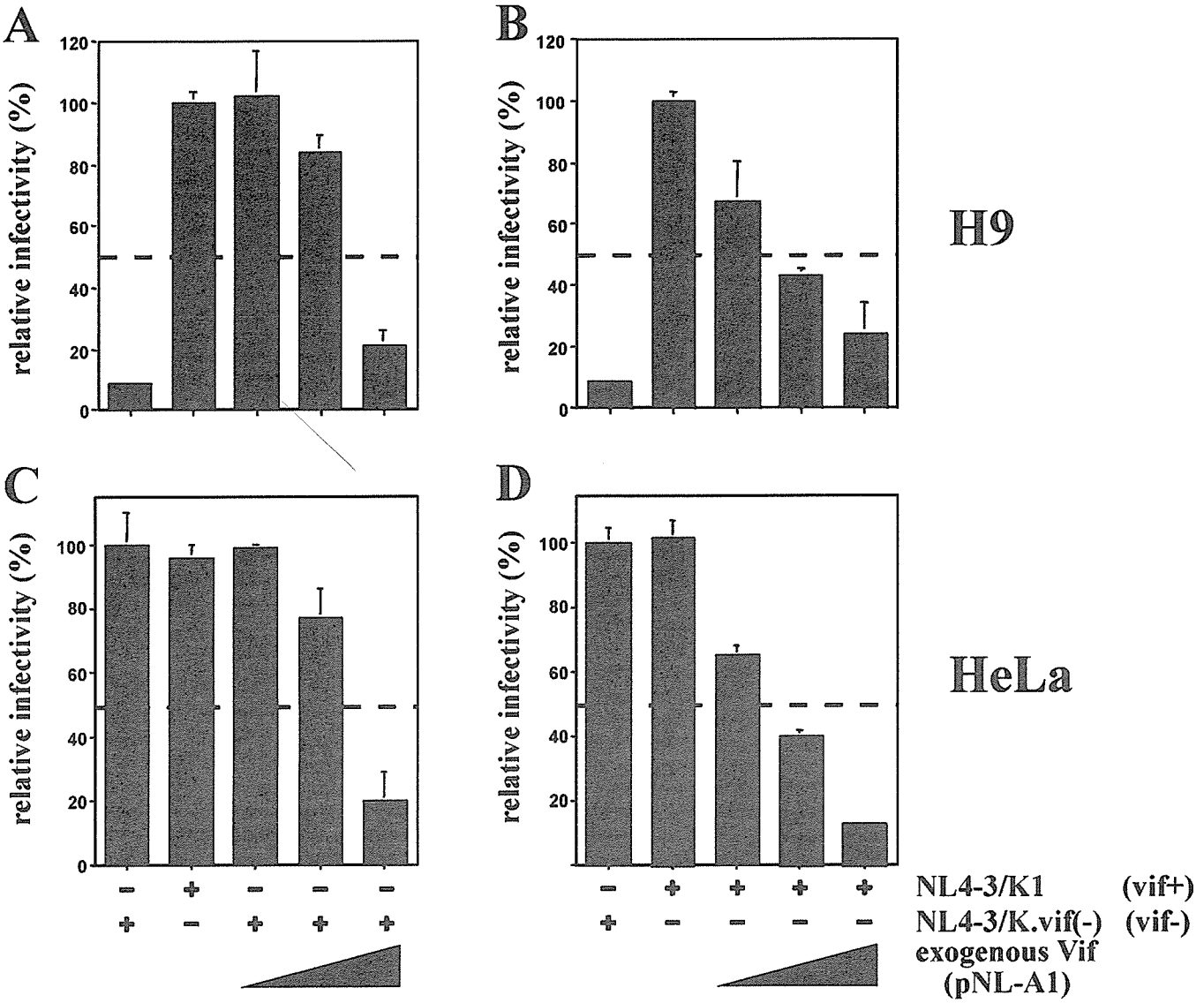

FIG. 3. **Inhibition of virus infectivity at high levels of Vif is cell type-independent.** *A* and *B*, H9 cells were electroporated with increasing amounts (1, 3, or 10 μg) of the Vif-expressing pNL-A1 plasmid DNA, together with a proviral construct and pHCMV-G, essentially as described for Fig. 1. In *A* the Vif- and Env-defective proviral vector pNL43-K1.vif(−) was employed, whereas in *B* a Vif-expressing variant, pNL43-K1, was used. *C* and *D*, HeLa cells were transfected following the same schedule as described for *A* and *B* except that the total amount of DNA was adjusted to 5 μg. The relative ratio of individual plasmids was not changed. Virus-containing supernatants were harvested for all samples 24 h after transfection, normalized for equal reverse transcriptase activity, and used for the infection of LuSIV cells. Viral infectivity was calculated as described for Fig. 1. In all four sets, a Vif-deficient control (*first bar* in each *panel*) and a positive control expressing physiological amounts of Vif (*second bar*) were included. The *dotted line* indicates 50% infectivity.

lower and higher levels of Vif are detrimental to virus infectivity.

Inhibition of Virus Infectivity at High Levels of Vif Is Cell Type-independent—The results from Fig. 2 are unexpected inasmuch as they are inconsistent with a model that simply envisions a role of Vif in the inactivation of cellular inhibitor(s) such as APOBEC3G. To directly examine the requirement of cellular inhibitory factors for the dose-dependent effect of Vif on viral infectivity, we compared the infectivity of virus stocks produced from non-permissive H9 cells and permissive HeLa cells in the presence of increasing amounts of Vif. In addition, to rule out the possibility that the inhibitory effect of Vif seen following overexpression in *trans* is due to the fact that the proviral vector employed in this study carried a defective *vif* gene, we analyzed a Vif-expressing variant (pNL43-K1) in direct comparison to the Vif-defective pNL43-K1.vif(−). H9 cells (Fig. 3, *A* and *B*) and HeLa cells (*C* and *D*) were transfected with increasing amounts (1–10 μg) of pNL-A1 together with fixed amounts (5 μg) of pNL43-K1 or pNL43-K1.vif(−) as indicated in Fig. 3. In addition, a fixed amount (5 μg) of pHCMV-G was included to produce VSV-G-pseudotyped virus stocks. As before, DNA quantities were adjusted to 20 μg in all samples using appropriate amounts of pNL-A1vif(−) plasmid DNA. Consistent with the results from Fig. 2, physiological levels of Vif supplied in *trans* or in *cis* produced fully infectious virus from both H9 and HeLa cells, and further increase in the amounts of Vif progressively reduced viral infectivity in H9-derived virus (Fig. 3, *A* and *B*). Interestingly, the inhibitory effect of Vif expressed in *cis* and in *trans* appeared to be additive because in the presence of endogenous Vif, smaller amounts of exogenous Vif were necessary for a comparable degree of inhibition (compare *A* and *B* of Fig. 3). These results indicate that the inhibitory effect of high levels of Vif on virus infectivity in Fig. 2 was not due to the lack of a functional *vif* gene.

Surprisingly, very similar results were observed when virus was produced from permissive HeLa cells (Fig. 3, *C* and *D*);

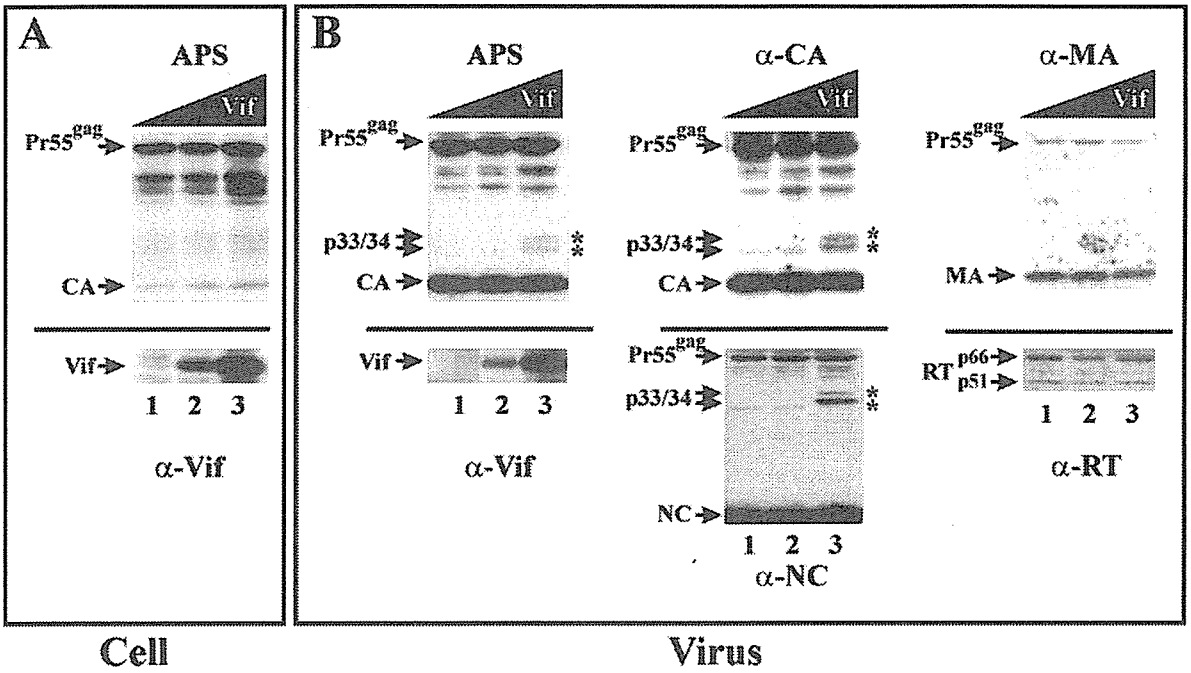

FIG. 4. **High level expression of Vif in H9-derived virus preparations reveals an effect of Vif on Gag maturation that is evident by the appearance of 33- and 34-kDa Gag intermediates.** H9 cells were cotransfected by electroporation with equal amounts of pNL43-K1.vif(−) and pNL-A1vif(−) (*lanes 1*), pNL43-K1 and pNL-A1vif(−) (*lanes 2*), or pNL43-K1 and pNL-A1 (*lanes 3*). Cell lysates (*A*) and viral pellets (*B*) obtained 24 h after transfection were analyzed for viral proteins by immunoblotting using an HIV-positive patient serum (*APS*) or antibodies against Vif (*α-Vif*), capsid (*α-CA*), nucleocapsid (*α-NC*), matrix (*α-MA*), and reverse transcriptase (*α-RT*) as indicated. Relative Vif expression levels are marked at the *top* of each *panel*. *Asterisks* mark the positions of the p33/34 Gag intermediates.

overexpression of Vif in *trans* reduced viral infectivity irrespective of the presence or absence of endogenous Vif. Again, endogenous Vif appeared to have an additive effect suggesting a similar molecular mechanism in both cell types. The fact that high level expression of Vif affected viral infectivity in the absence of cellular inhibitory factors suggests that this effect of Vif is unrelated to the noted inhibition of APOBEC3G and thus reflects a separate activity of Vif.

Vif Modulates Gag Processing during Virus Maturation—To investigate the molecular basis of the Vif-induced inhibition of viral infectivity, we performed a biochemical characterization of virions produced in the presence of varying amounts of Vif. The goal was to identify possible effects of Vif on Gag precursor processing or other effects on the viral protein composition that might explain the altered infectivity. In H9 cells, comparable expression and processing of viral proteins including $Pr55^{gag}$ and CA were detected intracellularly using an HIV-positive patient serum (Fig. 4*A*, *APS*) irrespective of the level of Vif expression (Fig. 4*A*, *α-Vif*). Interestingly, analysis of virus-associated proteins revealed two protein bands of ~33 and 34 kDa, respectively, that were apparent only in viruses produced in the presence of high levels of Vif (Fig. 4*B*, *APS*). Both proteins were also recognized by capsid- (Fig. 4*B*, *α-CA*) and nucleocapsid-specific (Fig. 4*B*, *α-NC*) antisera but not by a matrix-specific antibody (Fig. 4*B*, *α-MA*). The reactivity of p33/34 with CA- and NC-specific antibodies identified these proteins as Gag-processing intermediates composed of CA-p2-NC (p33) or CA-p2-NC-p1 (p34). The p33/34 intermediates were significantly less abundant than mature CA or NC suggesting that they represent a minor component of the virions. Importantly, processing of neither p66/p51 reverse transcriptase nor p17 MA was affected by the high levels of Vif (Fig. 4*B*), indicating that Vif does not act as a general PR inhibitor. In addition, similar Gag-processing intermediates were observed in virus derived from permissive HeLa cells in the presence of high levels of Vif (see Fig. 5). Together, the results

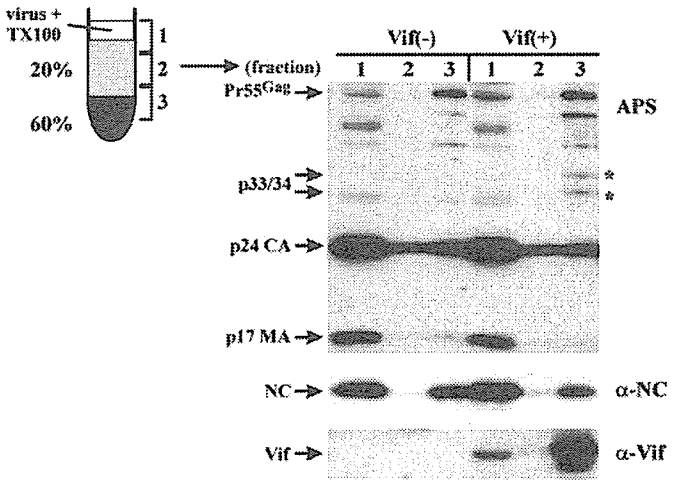

FIG. 5. **Vif and 33- and 34-kDa Gag intermediates copurify with the viral nucleoprotein complex.** HeLa cells were cotransfected with pNL4-3vif(−) and pNL-A1vif(−) (*Vif(−)*) or pNL4-3vif(−) and pNL-A1 (*Vif(+)*). Virus-containing supernatants were concentrated, adjusted to a final concentration of 0.1% Triton X-100, and subjected to sucrose step gradient centrifugation. Three equal fractions were collected as indicated in the diagram. Each fraction was analyzed for viral proteins by immunoblotting using an HIV-positive patient serum (*APS*) or antibodies to NC (*α-NC*) and Vif (*α-Vif*). *Asterisks* indicate the positions of p33/34.

from this experiment demonstrate that Vif modulates Gag processing to produce CA-p2-NC intermediates.

Vif and Gag Intermediates Associate with the Nucleoprotein Complex—Our observation that Vif modulates the maturation of Gag precursor molecules without acting as a general PR inhibitor suggests that Vif might inhibit Gag processing through steric interference. It is likely that such interference is caused by a direct interaction of Vif with the Gag precursor at or near the p2/NC cleavage site. In fact, several previous stud-

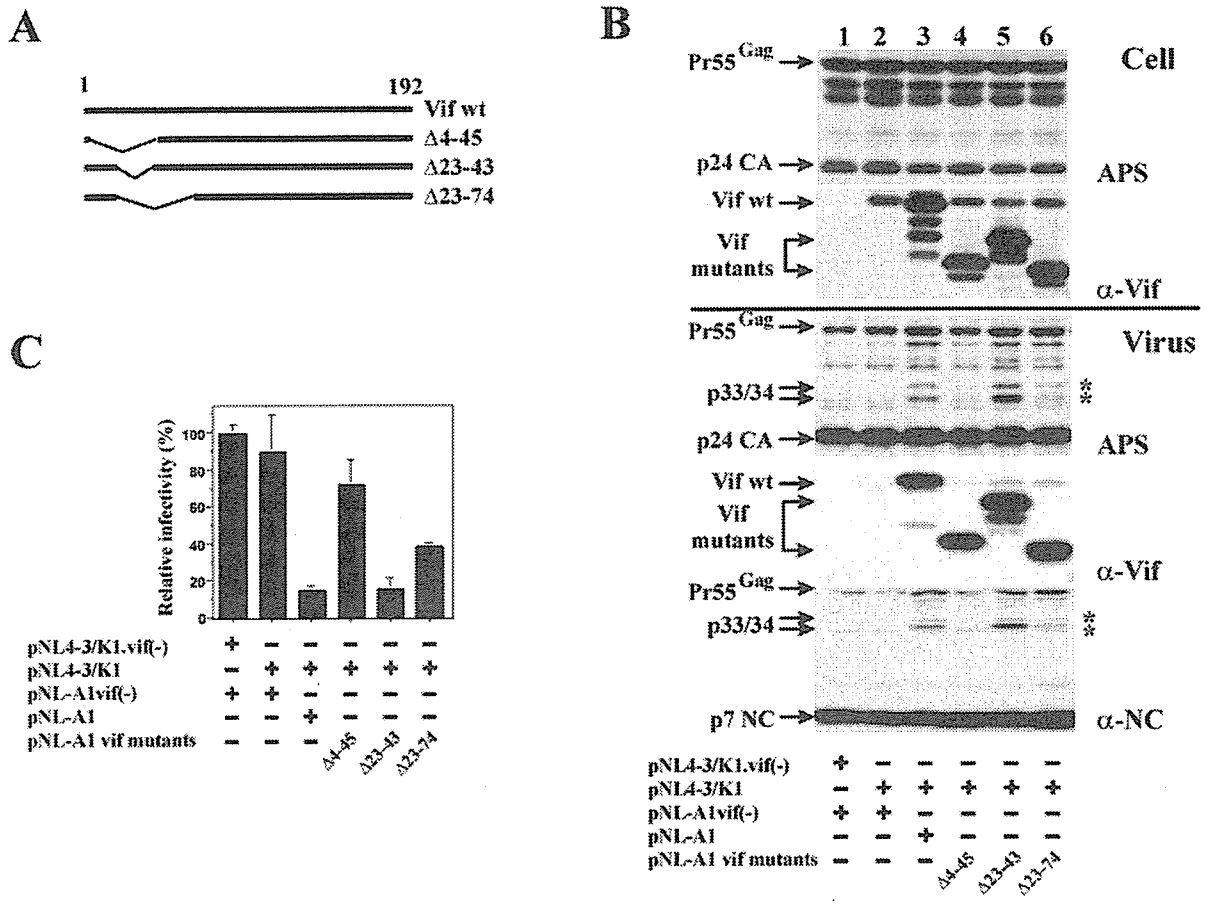

FIG. 6. **Effect of in-frame deletions on the ability of Vif to modulate maturation of Gag precursor molecules.** *A*, schematic diagram of Vif deletion mutants employed in this experiment. The amino acid regions deleted are shown on the *right*. *wt*, wild type. *B*, HeLa cells were cotransfected with equal amounts of pNL43-K1.vif(−) and pNL-A1vif(−) (*lane 1*), pNL43-K1 and pNL-A1vif(−) (*lane 2*), pNL43-K1 and pNL-A1 (*lane 3*), or pNL43-K1 and various pNL-A1-based Vif deletion mutants as indicated (*lanes 4–6*). Cell lysates (*Cell*) and concentrated virus preparations (*Virus*) were harvested 24 h after transfection and analyzed for viral proteins by immunoblotting using APS, anti-Vif, or anti-NC antibodies as indicated on the *right*. Viral proteins are identified on the *left*. *Asterisks* indicate the positions of p33/34. *C*, virus-containing supernatants from *B* were adjusted for equal reverse transcriptase activities and used for the infection of LuSIV indicator cells. Luciferase activity was determined as described under "Experimental Procedures," and the relative infectivity of the virus stocks was calculated.

ies have demonstrated direct interaction of Vif with the viral Gag precursor molecules *in vitro* (36–38). In addition, our recent observation that mutations in the NC zinc finger domains abolish Vif packaging further points to an interaction of Vif and NC (23). Also, virus-associated Vif is stably associated with the viral core, whereas major portions of the mature CA and NC are sensitive to detergent extraction and thus are either not or only loosely associated with the core (23). If maturation of Gag is blocked through steric interference by Vif, we would assume that the resulting intermediates colocalize with Vif in the viral core. To address this issue, viruses obtained from HeLa cells expressing high levels of Vif (Fig. 5, *Vif(+)*) or lacking Vif expression (Fig. 5, *Vif(−)*) were subjected to step gradient centrifugation in the presence of Triton X-100 as reported previously (23). Western blot analysis of individual fractions of the step gradient confirmed the stable association of Vif with the viral core in the insoluble fraction (Fig. 5, *lane 3*, *α-Vif*) as well as the presence of MA and major portions of CA and NC in the soluble fraction (Fig. 5, *lanes 1*). Interestingly, the p33/34 Gag intermediates were resistant to detergent extraction and colocalized with Vif in the viral core fraction (Fig. 5, *lane 3*, *asterisks*) in the presence of Vif. These findings indicate that unlike mature CA and NC products, the Gag p33/34 intermediates are tightly associated with the viral nucleoprotein complex, which also contains the viral genomic RNA, reverse transcriptase, integrase, residual $Pr55^{gag}$, and Vif (23).

Modulation of Gag Processing Requires Packaging of Vif and Involves N-terminal Regions in Vif—In an attempt to determine the domain(s) in Vif contributing to the modulation of proteolytic processing of the Gag precursor molecules, a series of Vif deletion mutants (schematically diagrammed in Fig. 6*A*) was evaluated. As can be seen in Fig. 6*B*, comparable amounts of the wild type and mutant Vif proteins were expressed intracellularly (Fig. 6*B*, *Cell*), indicating that the mutations did not affect steady-state levels of the resulting proteins. All Vif variants were packaged into virions at levels comparable with those of wild type virus (Fig. 6*B*, *Virus*, *α-Vif*). No aberrant Gag intermediates were apparent in the absence of Vif (Fig. 6*B*, *lane 1*, *APS*) or in the presence of physiological levels of Vif (*lane 2*, *APS* and *α-NC*). In contrast, high level expression of wild type Vif resulted in the appearance of the p33/34 intermediates (Fig. 6*B*, *lane 3*, *APS* and *α-NC*; marked by *asterisks*). Deletion of residues 23–43 in Vif did not impair the ability of Vif to modulate Gag processing as shown by the presence of p33/34 at levels comparable with those observed in the presence of wild type Vif (Fig. 6*B*, compare *lanes 3* and *5*, *Virus*, *APS* and *α-NC*). However, deletion of residues 4–45 (Fig. 6*B*, *lane 4*) completely abolished the ability of Vif to modulate Gag processing despite the presence of high levels of this Vif variant in the virus preparation. Finally, deletion of residues 23–74 (Fig. 6*B*, *lane 6*) partially inhibited the ability to modulate Gag maturation. We confirmed that none of these deletions affected the ability of Vif to associate with the nucleoprotein complex

(data not shown). Analysis of viral infectivity revealed an inverse correlation with the amounts of p33/34 detectable in the virus preparations (Fig. 6*C*). In contrast, there was no correlation between inhibition of viral infectivity and packaging of Vif. All Vif variants were expressed at similar levels and were packaged and associated with the viral nucleoprotein complex with similar efficiency. Taken together, these results support the notion that inhibition of virus infectivity is correlated with the presence of p33/34 Gag intermediates rather than with the amounts of Vif packaged. Our data further demonstrate that sequences in the N-terminal domain of Vif, in particular residues 4–22, are critical for the ability of Vif to inhibit Gag processing at the p2/NC site.

DISCUSSION

Despite the recent identification of a cellular factor whose inhibitory activity must be overcome by Vif to allow for the production of infectious viruses from non-permissive cell types (10), the molecular mechanism of Vif function and its site(s) of action have remained unclear. We now report for the first time on an activity of Vif that requires its presence in virus particles. Our data suggest that Vif modulates the maturation of a small number of Gag and/or Gag-Pol precursor molecules by physically interacting with the Gag or Gag-Pol precursor at or near the primary cleavage site. Such interaction causes the inhibition of or the delay in processing of Gag at the p2/NC cleavage site resulting in the accumulation of small amounts of p33/34 Gag-processing intermediates. Based on their reactivity with both CA- and NC-specific antibodies the p33/34 intermediates were identified as proteins consisting of CA, NC, and one or both of the spacer peptides p1 and p2. Vif did not affect processing at other proteolytic cleavage sites, suggesting that it selectively blocks processing at the CA-NC boundary through steric interference. It is interesting to note that Vif itself is a substrate for proteolytic processing (24), and it is possible that Vif blocks processing of Gag by acting as a decoy for the viral protease.

Processing of the Gag precursor occurs at five different sites to produce at least six mature processing products (39). This process is highly ordered and starts with an initial cleavage at the p2/NC boundary (40). The resulting processing intermediates are then further processed but at a much reduced rate (41). Inhibition of processing at any of the cleavage sites results in the production of non-infectious virions (41, 42). On the other hand, immunoblot analyses of normal infectious HIV-1 virions invariably identify a series of processing intermediates (see Figs. 2 and 6, *Virus, APS*; and 4, *α-CA*) that suggest that Gag processing is incomplete. Notably, most virus preparations contain residual uncleaved $Pr55^{gag}$ precursor. In fact, we noted previously that unlike most mature Gag products, $Pr55^{gag}$ is stably associated with the viral nucleoprotein complex (23). Thus, it is apparent that mature viral particles are composed not only of fully processed Gag and Gag-Pol products but contain residual amounts of Gag precursors and processing intermediates. Whether these processing intermediates have functional significance or are merely signs of an inefficient maturation process remains to be established. However, the noted affinity of $Pr55^{gag}$ as well as the p33/34 intermediates with the viral nucleoprotein complex could imply a role in its formation and/or stabilization.

Vif is known to enhance viral infectivity in a cell type-dependent manner. This phenomenon was recently attributed to the activity of the cellular cytidine deaminase APOBEC3G (13–17). APOBEC3G is packaged into HIV particles where it induces hypermutation of the minus-strand cDNA (10, 14–17). This inhibitory effect of APOBEC3G is counteracted by Vif, which interferes with the packaging of APOBEC3G. How Vif inhibits packaging of APOBEC3G is still under investigation; however, it appears to involve in part a reduction of the intracellular protein levels through proteasome-dependent degradation (18, 20, 21, 25, 35, 43) and requires a physical interaction between the two proteins (17, 18, 21, 35). Thus, like all other viral accessory proteins, Vif appears to be a multifunctional adapter molecule with seemingly opposing effects; binding of Vif to APOBEC3G appears to accelerate its intracellular turnover, whereas the interaction of Vif with the Gag precursor in virions inhibits its proteolytic processing. It is currently unclear whether the domains in Vif required for interaction with APOBEC3G and Gag are the same or map to different regions in the protein. The results from our current study (Fig. 6) suggest that inhibition of Gag processing involves an N-terminal domain in Vif. Although these same mutants were found to also be inactive with respect to APOBEC3G (19), other Vif mutants such as VifΔ23–43 were inactive against APOBEC3G (19) but still inhibited Gag maturation. These results combined with the fact that the effect of Vif on the proteolytic processing of Gag precursors is cell type-independent suggest that the effect of Vif on Gag maturation is mechanistically independent of its neutralization of APOBEC3G. It remains to be investigated whether the interaction of Vif with Gag precursor molecules during or following virus assembly relates to its ability to inhibit packaging of APOBEC3G. This seems possible as the reported reduction of intracellular expression levels of APOBEC3G by Vif does not fully account for the noted exclusion of APOBEC3G from virus particles (17, 19).

The fact that high level expression of Vif is detrimental to viral infectivity confirms that Gag maturation is a carefully balanced process. Thus, rapid degradation of Vif in virus-producing cells may have evolved as a mechanism to preclude the detrimental effects on Gag maturation. Our observation that the accumulation of the CA-p2-NC intermediates is directly correlated with the levels of Vif expression (data not shown) leads us to conclude that similar processing intermediates are produced under physiological conditions but are below the limit of detection in our assay system. The fact that packaging of large quantities of Vif N-terminal deletion mutants did not affect Gag maturation (Fig. 6) suggests that the effect of Vif is specific albeit only detectable by currently available immunoblotting techniques at high levels of Vif. Thus, it is possible that minute quantities of CA-p2-NC- and CA-p2-NC-p1-processing intermediates play an important role in viral infectivity. The fact that such intermediates, unlike their mature products, are stably associated with the nucleoprotein complex raises the possibility that the association of these intermediates with Vif and viral genomic RNA promotes the stability or proper conformation of the viral nucleoprotein complex. Such a function would be consistent with previous reports correlating the lack of Vif with a reduced stability of nucleoprotein complexes (8, 44, 45).

Acknowledgments—We thank Stephan Bour and Eri Miyagi for helpful discussions and Eric Freed for critical comments on the manuscript. We thank Alicia Buckler-White and Ron Plishka for oligonucleotide synthesis and sequence analysis. We acknowledge Mary Karczewski and Claudia Aberham for construction of the Vif mutants and Robert Gorelick, Susan Zolla-Pazner, and Paul Spearman for antibodies. Antibodies to CA and MA were obtained through the National Institutes of Health AIDS Research and Reference Reagent Program.

REFERENCES

1. Bour, S., and Strebel, K. (2000) *Adv. Pharmacol.* **48,** 75–120
2. Cullen, B. R. (1998) *Cell* **93,** 685–692
3. Akari, H., Uchiyama, T., Fukumori, T., Iida, S., Koyama, A. H., and Adachi, A. (1999) *J. Gen. Virol.* **80,** 2945–2949
4. Chowdhury, I. H., Chao, W., Potash, M. J., Sova, P., Gendelman, H. E., and Volsky, D. J. (1996) *J. Virol.* **70,** 5336–5345
5. Courcoul, M., Patience, C., Rey, F., Blanc, D., Harmache, A., Sire, J., Vigne, R., and Spire, B. (1995) *J. Virol.* **69,** 2068–2074
6. Goncalves, J., Korin, Y., Zack, J., and Gabuzda, D. (1996) *J. Virol.* **70,**

8701–8709
7. Reddy, T. R., Kraus, G., Yamada, O., Looney, D. J., Suhasini, M., and Wong-Staal, F. (1995) *J. Virol.* **69,** 3549–3553
8. Simon, J. H., and Malim, M. H. (1996) *J. Virol.* **70,** 5297–5305
9. von Schwedler, U., Song, J., Aiken, C., and Trono, D. (1993) *J. Virol.* **67,** 4945–4955
10. Sheehy, A. M., Gaddis, N. C., Choi, J. D., and Malim, M. H. (2002) *Nature* **418,** 646–650
11. Madani, N., and Kabat, D. (1998) *J. Virol.* **72,** 10251–10255
12. Simon, J. H., Gaddis, N. C., Fouchier, R. A., and Malim, M. H. (1998) *Nat. Med.* **4,** 1397–1400
13. Harris, R. S., Bishop, K. N., Sheehy, A. M., Craig, H. M., Petersen-Mahrt, S. K., Watt, I. N., Neuberger, M. S., and Malim, M. H. (2003) *Cell* **113,** 803–809
14. Zhang, H., Yang, B., Pomerantz, R. J., Zhang, C., Arunachalam, S. C., and Gao, L. (2003) *Nature* **424,** 94–98
15. Mangeat, B., Turelli, P., Caron, G., Friedli, M., Perrin, L., and Trono, D. (2003) *Nature* **424,** 99–103
16. Lecossier, D., Bouchonnet, F., Clavel, F., and Hance, A. J. (2003) *Science* **300,** 1112
17. Mariani, R., Chen, D., Schrofelbauer, B., Navarro, F., Konig, R., Bollman, B., Munk, C., Nymark-McMahon, H., and Landau, N. R. (2003) *Cell* **114,** 21–31
18. Stopak, K., de Noronha, C., Yonemoto, W., and Greene, W. C. (2003) *Mol. Cell* **12,** 591–601
19. Kao, S., Khan, M. A., Miyagi, E., Plishka, R., Buckler-White, A., and Strebel, K. (2003) *J. Virol.* **77,** 11398–11407
20. Sheehy, A. M., Gaddis, N. C., and Malim, M. H. (2003) *Nat. Med.* **9,** 1404–1407
21. Marin, M., Rose, K. M., Kozak, S. L., and Kabat, D. (2003) *Nat. Med.* **9,** 1398–1403
22. Kao, S., Akari, H., Khan, M. A., Dettenhofer, M., Yu, X. F., and Strebel, K. (2003) *J. Virol.* **77,** 1131–1140
23. Khan, M. A., Aberham, C., Kao, S., Akari, H., Gorelick, R., Bour, S., and Strebel, K. (2001) *J. Virol.* **75,** 7252–7265
24. Khan, M. A., Akari, H., Kao, S., Aberham, C., Davis, D., Buckler-White, A., and Strebel, K. (2002) *J. Virol.* **76,** 9112–9123
25. Yu, X., Yu, Y., Liu, B., Luo, K., Kong, W., Mao, P., and Yu, X. F. (2003) *Science* **302,** 1056–1060
26. Adachi, A., Gendelman, H. E., Koenig, S., Folks, T., Willey, R., Rabson, A., and Martin, M. A. (1986) *J. Virol.* **59,** 284–291
27. Bour, S., and Strebel, K. (1996) *J. Virol.* **70,** 8285–8300
28. Karczewski, M. K., and Strebel, K. (1996) *J. Virol.* **70,** 494–507
29. Yee, J. K., Miyanohara, A., LaPorte, P., Bouic, K., Burns, J. C., and Friedmann, T. (1994) *Proc. Natl. Acad. Sci. U. S. A.* **91,** 9564–9568
30. Strebel, K., Daugherty, D., Clouse, K., Cohen, D., Folks, T., and Martin, M. A. (1987) *Nature* **328,** 728–730
31. Gorny, M. K., Gianakakos, V., Sharpe, S., and Zolla-Pazner, S. (1989) *Proc. Natl. Acad. Sci. U. S. A.* **86,** 1624–1628
32. Varthakavi, V., Browning, P. J., and Spearman, P. (1999) *J. Virol.* **73,** 10329–10338
33. Roos, J. W., Maughan, M. F., Liao, Z., Hildreth, J. E., and Clements, J. E. (2000) *Virology* **273,** 307–315
34. Aiken, C. (1997) *J. Virol.* **71,** 5871–5877
35. Mehle, A., Strack, B., Ancuta, P., Zhang, C., McPike, M., and Gabuzda, D. (2004) *J. Biol. Chem.* **279,** 7792–7798
36. Bardy, M., Gay, B., Pebernard, S., Chazal, N., Courcoul, M., Vigne, R., Decroly, E., and Boulanger, P. (2001) *J. Gen. Virol.* **82,** 2719–2733
37. Bouyac, M., Courcoul, M., Bertoia, G., Baudat, Y., Gabuzda, D., Blanc, D., Chazal, N., Boulanger, P., Sire, J., Vigne, R., and Spire, B. (1997) *J. Virol.* **71,** 9358–9365
38. Huvent, I., Hong, S. S., Fournier, C., Gay, B., Tournier, J., Carriere, C., Courcoul, M., Vigne, R., Spire, B., and Boulanger, P. (1998) *J. Gen. Virol.* **79,** 1069–1081
39. Henderson, L. E., Sowder, R. C., Copeland, T. D., Oroszlan, S., and Benveniste, R. E. (1990) *J. Med. Primatol.* **19,** 411–419
40. Erickson-Viitanen, S., Manfredi, J., Viitanen, P., Tribe, D. E., Tritch, R., Hutchison, C. A., III, Loeb, D. D., and Swanstrom, R. (1989) *AIDS Res. Hum. Retroviruses* **5,** 577–591
41. Pettit, S. C., Moody, M. D., Wehbie, R. S., Kaplan, A. H., Nantermet, P. V., Klein, C. A., and Swanstrom, R. (1994) *J. Virol.* **68,** 8017–8027
42. Wiegers, K., Rutter, G., Kottler, H., Tessmer, U., Hohenberg, H., and Krausslich, H. G. (1998) *J. Virol.* **72,** 2846–2854
43. Conticello, S. G., Harris, R. S., and Neuberger, M. S. (2003) *Curr. Biol.* **13,** 2009–2013
44. Ohagen, A., and Gabuzda, D. (2000) *J. Virol.* **74,** 11055–11066
45. Hoglund, S., Ohagen, A., Lawrence, K., and Gabuzda, D. (1994) *Virology* **201,** 349–355
46. Willey, R. L., Smith, D. H., Lasky, L. A., Theodore, T. S., Earl, P. L., Moss, B., Capon, D. J., and Martin, M. A. (1988) *J. Virol.* **62,** 139–147

Available online at www.sciencedirect.com
SCIENCE DIRECT
Journal de pédiatrie et de puériculture 6 (2004) 791–798
Microbes and Infection
www.elsevier.com/locate/micinf

Original article

Expression of HIV-1 accessory protein Vif is controlled uniquely to be low and optimal by proteasome degradation

Mikako Fujita [a,*], Hirofumi Akari [b], Akiko Sakurai [a], Akiko Yoshida [a], Tomoki Chiba [c], Keiji Tanaka [c], Klaus Strebel [d], Akio Adachi [a]

[a] *Department of Virology, The University of Tokushima, Graduate School of Medicine, 3-18-15 Kuaramoto-cho, Tokushima-shi Tokushima 770-8503, Japan*
[b] *Tsukuba Primate Center for Medical Sciences, National Institute of Infectious Diseases, Tsukuba, Ibaraki 305-0843, Japan*
[c] *Tokyo Metropolitan Institute of Medical Science, Bunkyo-ku, Tokyo 113-8613, Japan*
[d] *Laboratory of Molecular Microbiology, National Institute of Allergy and Infectious Diseases, Bethesda, MD 20892-0460, USA*

Received 29 March 2004; accepted 13 April 2004

Available online 07 June 2004

Abstract

While the Vif protein of human immunodeficiency virus type 1 (HIV-1) is essential for viral replication in non-permissive cells, it is rapidly degraded intracellularly. We have previously suggested that the rapid turn-over of Vif is biologically meaningful to prevent detrimental effects of this protein at high expression levels. We now studied the mechanism of Vif degradation by examining the blocking effect of protease inhibitors in pulse/chase experiments and by monitoring the extent of Vif ubiquitination. The rapid turn-over of Vif could be blocked by proteasome inhibitors, and Vif was highly ubiquitinated. Cytoskeletal Vif was found to be more stable than soluble cytosolic Vif. These degradation characteristics of Vif were cell type-independent and observed in both non-permissive and permissive cells. Characterization of a series of *vif* deletion mutants showed that amino acids predicted to be important for formation of β-strand structures (amino acid nos. 63–70 and 86–89) were critical for maintaining a normal expression level of Vif and for viral infectivity. Finally, we performed comparative stability analysis of the four HIV-1 accessory proteins. Vif was unique in its short half-life and in the magnitude of the degradation. Taken together, we conclude that the proteasome degradation of HIV-1 Vif is a virologically important process and crucial for the function of Vif.

Keywords: HIV-1; Vif; Proteasome degradation; Accessory proteins

1. Introduction

The Vif protein of HIV-1 is encoded by an accessory gene that is conserved in all known lentiviruses, except for equine infectious anemia virus [1], and is indispensable for viral replication in a certain type of cell (for review, see Refs. [2–5]). It acts during the stage of assembly, budding, or maturation to greatly augment the infectivity of progeny virions in a producer cell-dependent manner. Producer cells are, therefore, divided into permissive and non-permissive, and HIV-1 grown in non-permissive cells like primary human T cells and a restricted number of cell lines such as H9 and CEM is unable to replicate in any type of target cells in the absence of Vif. Many cell lines, such as 293T and HeLa, are classified as permissive cells. Previous studies suggested that Vif counteracts certain cellular anti-HIV-1 factor(s) present in non-permissive cells [6,7]. Indeed, the recent identification of APOBEC3G (CEM15) as a cellular inhibitor of HIV-1 replication [8] confirmed this speculation on the existence of an inhibitory factor in non-permissive cell types. APOBEC3G was subsequently found to deaminate dC to dU in the newly synthesized minus strand DNA of HIV-1, resulting in G to A hypermutation of the viral plus strand DNA [9–12]. However, the mechanism by which Vif overcomes the function of APOBEC3G remains unclear. Some reports show that Vif induces proteasome-dependent degradation of APOBEC3G [13–16] while others report an effect on APOBEC3G translation [17,18] or both [19]. The precise degradation profile of Vif itself remains to be determined.

* Corresponding author. Tel.: +81-88-633-9232; fax: +81-88-633-7080.
E-mail address: mfujita@basic.med.tokushima-u.ac.jp (M. Fujita).

1286-4579/$ - see front matter © 2004 Elsevier SAS. All rights reserved.
doi:10.1016/j.micinf.2004.04.011

We have previously shown that Vif is rapidly decayed both in the absence and presence of APOBEC3G in transiently transfected HeLa cells, and that expression of Vif to an excessive level is inhibitory to viral replication [20]. In the current study we report that newly synthesized Vif is rapidly and similarly degraded in transiently transfected 293T, HeLa and H9 cells. We found that Vif present in detergent-resistant compartments was more stable than soluble cytosolic Vif. Treatment of 293T cells with proteasome inhibitors but not with inhibitors of lysosome degradation and the calpain system blocked the degradation of Vif. In fact, Vif was highly polyubiquitinated in the cells. We investigated the structural basis of stable expression of Vif by deletion analysis and found that amino acids in the predicted β-strand structures (amino acid nos. 63–70 and 86–89 in Vif) are critically important for a normal expression level of Vif and for viral infectivity. We further examined and compared the stability of all four HIV-1 accessory proteins. Rapid turn-over was demonstrated to be unique to Vif among the viral proteins tested. These results show that expression of Vif is controlled to be limited and optimal by proteasome degradation, and suggest that HIV-1 has apparently evolved to regulate Vif levels to suit its requirements for efficient replication and spread.

2. Materials and methods

2.1. Plasmids

The full-length molecular clone pNL432 was used for production of wild-type (wt) infectious virus [21]. Construction and characterization of proviral deletion mutants designated pNL-fE88*del*, -fW89*del*, -fR90*del*, -fK91*del*, -fK92*del*, and -fR93*del* have been previously described [22]. New proviral deletion mutants designated pNL-fL64*del*, -fV65*del*, -fI66*del*, and -fT67*del*, -fS86*del*, and -fI87*del* were constructed from pNL432 by the QuikChange site-directed mutagenesis kit (Stratagene, La Jolla, CA, USA) as previously described [22,23]. For efficient expression of wt Vif, the subgenomic expression vector pNL-A1 [24] was used. A pNL-A1 version of mutant Vif (E88*del*) expression vector designated pNLA1-E88*del* was constructed by insertion of the *Nde*I-*Eco*RI fragment of pNL-fE88*del* into the *Nde*I and *Eco*RI sites of pNL-A1. An HIV-1 Gag-p24 expression vector pSG-Gag (p24) cFLAG was constructed from pcDNA3 (Invitrogen Corp., Carlsbad, CA, USA) carrying FLAG (pcDNA3cFLAG) and pSG5 (Stratagene, La Jolla, CA, USA). The ubiquitin expression vector pcDNA3.1-HA-Ub constructed from pcDNA3.1 (Invitrogen, Corp., Carlsbad, CA, USA) [25] was used to monitor the ubiquitination of Vif.

2.2. Cells

H9 [26] cells were cultured in RPMI-1640 medium supplemented with 10% heat-inactivated fetal bovine serum (FBS). The 293T [27] and HeLa (ATCC CCL-2) cells were cultured in Dulbecco's modified Eagle medium supplemented with 10% heat-inactivated FBS.

2.3. Transfection

For transfection of H9 cells, the electroporation method was used, as previously described [21]. For transfection of HeLa and 293T cells, the calcium-phosphate coprecipitation method [21] or the LipofectAMINE PLUS™ system (Invitrogen Corp., Carlsbad, CA, USA) was used.

2.4. Pulse/chase analysis of viral proteins

Transfected cells were metabolically labeled for 5 min with the Redivue Pro-mix L-[^{35}S] in vitro cell labeling mix system (Amersham Biosciences Corp., Piscataway, NJ, USA). After the labeling, cells were pelleted and suspended in complete RPMI containing all amino acids and 10% FBS. Cells were incubated for various times at 37 °C as indicated in the text. Cells were then pelleted and stored at –80 °C. Cell pellets were subsequently extracted with CHAPS buffer (50 mM Tris–HCl, pH 8.0, 5 mM EDTA, 100 mM NaCl, and 0.5% (v/v) CHAPS (3-[(3-cholamidopropyl)dimethylammonio]-1-propanesulfonate)) supplemented with 0.2% deoxycholate (DOC), incubated on ice for 5 min, vortexed, and pelleted for 3 min at 15000 × *g*. Proteins in the supernatant were designated sol (soluble fraction). Proteins present in the pellet were solubilized by dissolving in PBS–Laemmli's sample buffer (1:1) and heating at 95 °C for 30 min. The solution was then centrifuged for 3 min at 15000 × *g*. Proteins in the resultant supernatant were designated insol (insoluble fraction). These two fractions were used for immunoprecipitation with a specific antibody. Immunoprecipitated proteins were solubilized by boiling in the sample buffer and separated by SDS-PAGE. Radioactive bands were visualized by fluorography and quantitated by scanning.

2.5. Western immunoblot analysis of viral proteins

Transfected 293T cells were collected and solubilized by the CHAPS/DOC method as above or by dissolving directly into Laemmli's sample buffer. For some experiments, cells collected were suspended in PBS, subjected to two cycles of freeze–thaw, and pelleted for 3 min at 15000 × *g*. Proteins in the supernatant were designated sol-1. Proteins in the pellet were solubilized by the CHAPS/DOC and pelleted for 3 min at 15000 × *g*. The resultant supernatant was designated sol-2. Proteins present in the pellet were solubilized by dissolving in PBS–Laemmli's sample buffer (1:1) and heating at 95 °C for 30 min. The solution was then centrifuged for 3 min at 15000 × *g*. Proteins in the resultant supernatant were designated insol. Protein samples were resolved by SDS-PAGE followed by electrophoretic transfer to polyvinylidene fluoride membranes. The membranes were treated with specific antibodies and visualized with the ECL plus Western Blot-

ting Detection System (Amersham Biosciences UK Limited, Buckinghamshire, England), as previously described [22,23].

2.6. Immunoprecipitation/western blot analysis of Vif ubiquitination

The 293T cells were transfected with pNL-A1, pcDNA3.1-HA-Ub or pNL-A1 plus pcDNA3.1-HA-Ub, and cultured for 48 h. Transfected cells were cultured in the presence of MG-132 (50 μM) during the last incubation period, as indicated in the text. Cells were collected, lysed by TNE buffer (10 mM Tris–HCl pH 7.8, 0.15 M NaCl, 1 mM EDTA, 1% NP40, 10 μg/ml of aprotinin) and immunoprecipitated with a polyclonal anti-Vif antibody (no. 2221 of NIH AIDS Research and Reference Reagent Program Catalog). The precipitated proteins were analyzed by western blotting using a monoclonal anti-HA antibody HA.11 (BabCO, Berkeley, CA, USA).

2.7. Reverse transcriptase (RT) assay

Virion-associated RT activity was determined as previously described [28].

3. Results

3.1. Vif is rapidly degraded by proteasomes in a cell-type-independent manner

Recent work by us has indicated that soluble cytosolic Vif is rapidly degraded in HeLa cells both in the absence and presence of APOBEC3G [20]. Extensive analysis of subcellular localization of Vif has demonstrated the existence of a soluble and a cytoskeletal form, and to a much lesser extent, the presence of a detergent-extractable form of Vif [29]. We first asked whether insoluble cytoskeletal Vif is unstable and whether the rapid degradation of Vif is generally observed in various cell types. We also asked whether the degradation can be blocked by proteasome inhibitors [30,31]. To address these questions, we performed pulse/chase and western blot analyses in transiently transfected 293T cells (Fig. 1). Vif was expressed from the subgenomic vector pNL-A1 [24], which is known to produce a high level of Vif upon transfection. Transfected 293T cells were labeled for 5 min with [^{35}S]-methionine and [^{35}S]-cysteine, chased for up to 60 min in the absence or presence of MG-132, and used for cell fractionation studies, as described in Section 2. As shown in Fig. 1A and B, while cytosolic Vif was degraded rapidly, cytoskeletal Vif was quite stable and accumulated with time. The proteasome inhibitor MG-132 blocked significantly the degradation of cytosolic Vif. This blocking effect was not observed for inhibitors of lysosome degradation (Bafilomycin A1 and EST) and calpain system (calpeptin) (data not shown). Accumulation of cytoskeletal Vif in cells was con-

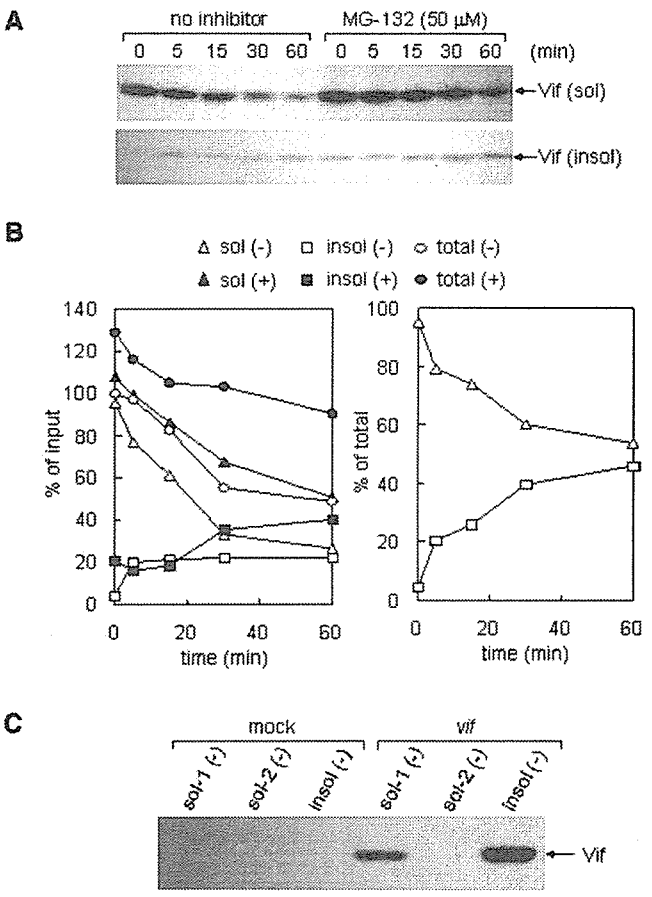

Fig. 1. Stability analysis of HIV-1 Vif in 293T cells. (A) Stability of Vif in the absence or presence of proteasome inhibitor MG-132. 293T cells were transfected with 5 μg of pNL-A1. Cells were collected 24 h after transfection, labeled for 5 min with [^{35}S]-methionine and [^{35}S]-cysteine, and chased for up to 60 min, as indicated above the lanes. Cells were incubated in the presence of MG132 (50 μM) during the labeling and chasing time where indicated. Cell lysates were prepared as described in Section 2 and precipitated with a Vif-specific polyclonal antibody Vif93 [29]. Vif proteins were identified by SDS-PAGE followed by fluorography; sol: soluble fraction; insol: insoluble fraction. (B) Degradation kinetics of Vif. Vif-specific bands in (A) were quantified by scanning, and relative values were plotted as a function of time; (–), absence of MG-132; (+), presence of MG-132; total: sol plus insol. (C) Steady-state expression of Vif. 293T cells were transfected with 5 μg of pNL-A1 (*vif*) or pUC19 (mock). Cells were harvested at 40 h post-transfection, and cell lysates were prepared as described in Section 2 for western blot analysis using an antibody Vif93. For sol-1, sol-2 and insol, see Section 2.

firmed by western blot analysis of transfected 293T cells at 40 h post-transfection (Fig. 1C). We extended these analyses to H9 and HeLa cells (Fig. 2). Transfected H9 and HeLa cells were pulse-labeled and chased as described above, and the degradation kinetics of two forms of Vif were monitored. As shown in Fig. 2, whereas Vif of a soluble form was degraded similarly rapidly, Vif of an insoluble form was quite stable and accumulated as observed in 293T cells.

Based on the effects of MG-132, Bafilomycin A1, EST, and calpeptin, we next assessed whether the ubiquitin–proteasome pathway was required for Vif degradation. Proteins that are selected for proteasomal degradation are marked by polyubiquitination (for review, see Refs. [32,33]). We co-

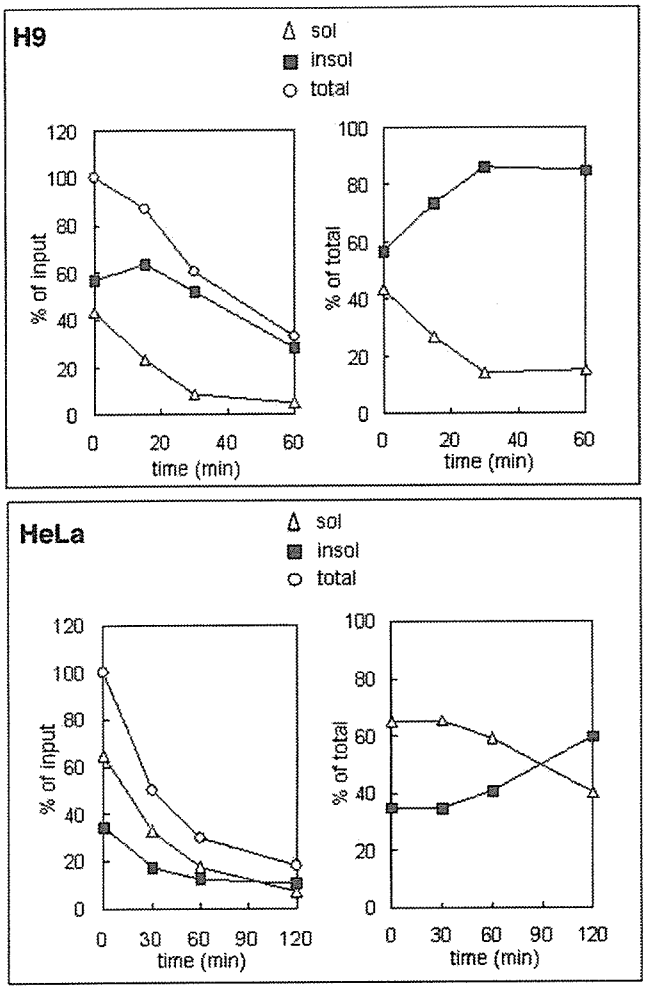

Fig. 2. Stability analysis of HIV-1 Vif in H9 and HeLa cells. Cells were transfected with 10 μg of pNL-A1 plus 10 μg of pNL432 (H9) or 5 μg of pNL-A1 (HeLa). Cells were collected 24 h after transfection, labeled for 5 min with [^{35}S]-methionine and [^{35}S]-cysteine, and chased for up to 60 min, as indicated. Cell lysates were prepared as described in Section 2 and precipitated with a Vif-specific polyclonal antibody Vif93 [29]. Vif proteins were identified by SDS-PAGE followed by fluorography. Vif-specific bands were quantified by scanning, and relative values were plotted as a function of time; sol: soluble fraction; insol: insoluble fraction; total: sol plus insol.

transfected 293T cells with pNL-A1 and a vector that expresses HA-tagged ubiquitin, and the cells were analyzed by immunoprecipitation/western blot, as described in Section 2. As shown in Fig. 3, co-transfected cells contained large polyubiquitinated Vif proteins in amounts that were increased by prolonged incubation time with the proteasome inhibitor MG-132.

3.2. Formation of β-strand structures is important for regulated expression and function of Vif

We have recently shown that amino acid residues 88 and 89 in NL432 Vif are critical for steady-state expression of Vif and for viral infectivity [22]. The two residues are located within a β-strand structure (residues 86–89) as predicted by the PredictProtein (http://www.embl-heidelberg.de/predictprotein/predictprotein.html). We wanted to evaluate

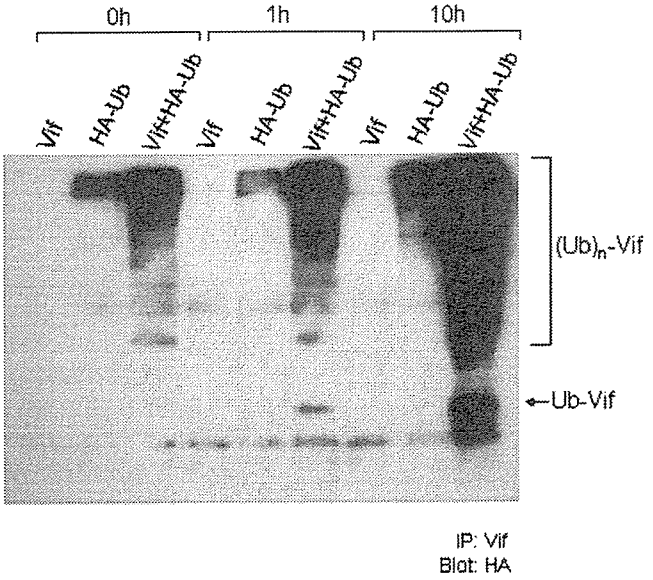

Fig. 3. Ubiquitination of HIV-1 Vif. 293T cells were singly transfected with 3 μg of pNL-A1 (Vif) or pcDNA3.1-HA-Ub (HA-Ub), or were double-transfected with pNL-A1 (1.5 μg) plus pcDNA3.1-HA-Ub (1.5 μg) (Vif + HA-Ub), and cultured for 48 h. Cells were cultured in the presence of MG-132 (50 μM) during the last incubation period, as indicated above the lanes. Cell lysates were prepared, immunoprecipitated with a polyclonal anti-Vif antibody (NIH catalog no. 2221), and the precipitated proteins were analyzed by western blotting using a monoclonal anti-HA antibody HA.11 (BAbCO, Berkeley, CA, USA), as described in Section 2. $(Ub)_n$-Vif, polyubiquitinated Vif; Ub-Vif, monoubiquitinated Vif; IP:Vif, immunoprecipitation by anti-Vif antibody; Blot:HA, western blot analysis using anti-HA antibody.

the importance of the amino acids in this β-strand and in an adjacent one (residues 63–70) for Vif expression and for viral infectivity by deletion analysis (Fig. 4). Proviral deletion mutants designated pNL-fL64*del*, -fV65*del*, -fI66*del*, -fT67*del*, -fS86*del* and -fI87*del* were newly constructed from pNL432, as described in Section 2. Various proviral clones were transfected into 293T and H9 cells and monitored for expression of Vif and for viral infectivity, respectively. As shown in Fig. 4A, amino acids within the β-strand structures, but not those on the outside, were indispensable for normal expression of Vif in 293T cells. Growth potentials of the deletion mutants in H9 cells were then monitored. As shown in Fig. 4B, the mutants, which express Vif at a very low level in 293T cells, were not infectious for H9 cells. We then determined whether the observed low expression level of mutant Vif is due to rapid degradation rate. A pNL-A1 version of mutant Vif (pNLA1-E88*del*) was constructed, and pulse/chase experiments using 293T cells were carried out, as described above. As can be clearly seen in Fig. 5A and B, E88*del* mutant Vif was more rapidly degraded than wt Vif. To ascertain the effect of proteasome inhibitors MG-132 and *clasto*-lactacystin β-lactone [30,31], steady-state levels of wt and mutant Vif proteins expressed by full-length proviral clones were determined in transfected 293T cells in the presence or absence of the inhibitors. As shown in Fig. 5C, E88*del* mutant Vif was expressed at a level similar to that of wt Vif only when the inhibitors were present.